Experimental study of QCD phase diagram at NICA energy range

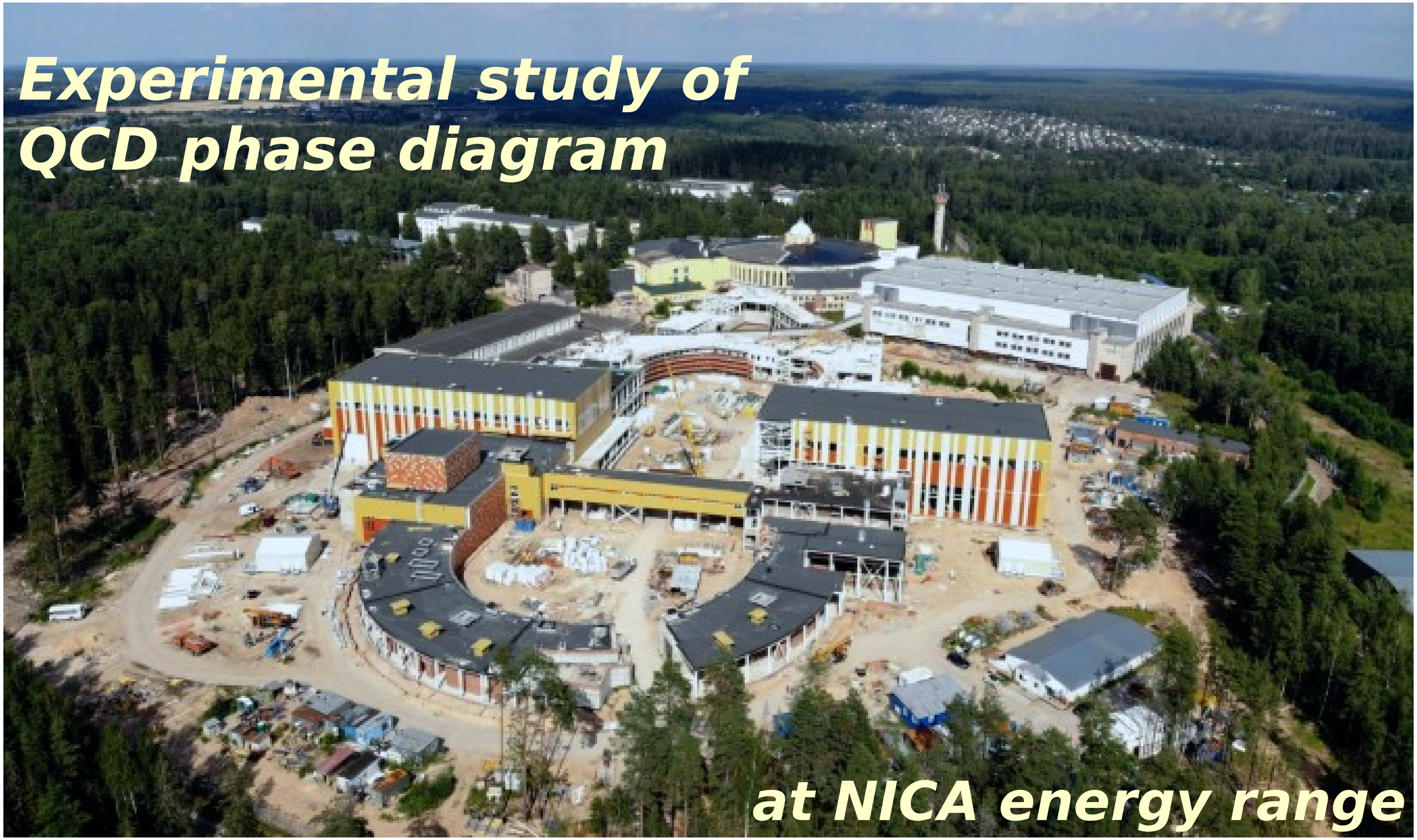

Rogachevsky Oleg

HPSI
Nov. 13 2020
Protvino

QCD phase diagram

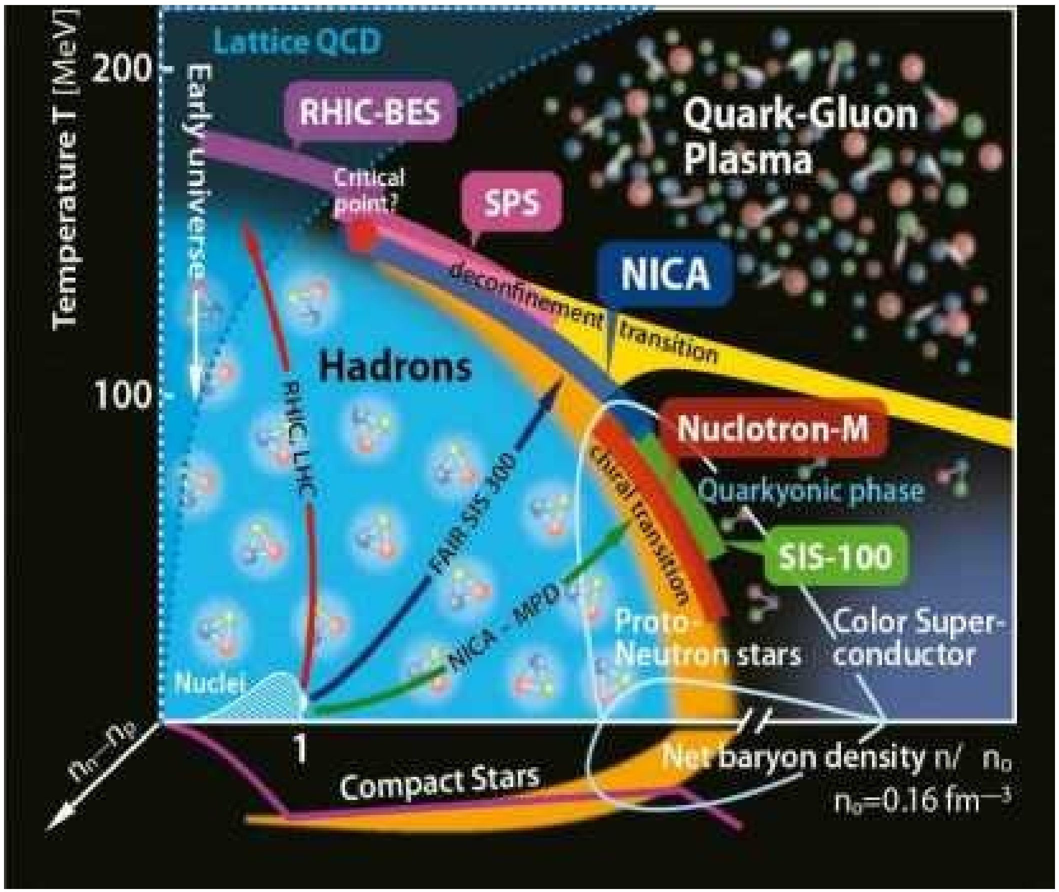

M. Stephanov

XXIV International Symposium on Lattice Field Theory
July 23-28 2006
Tucson Arizona, US
arXiv:hep-lat/0701002v1

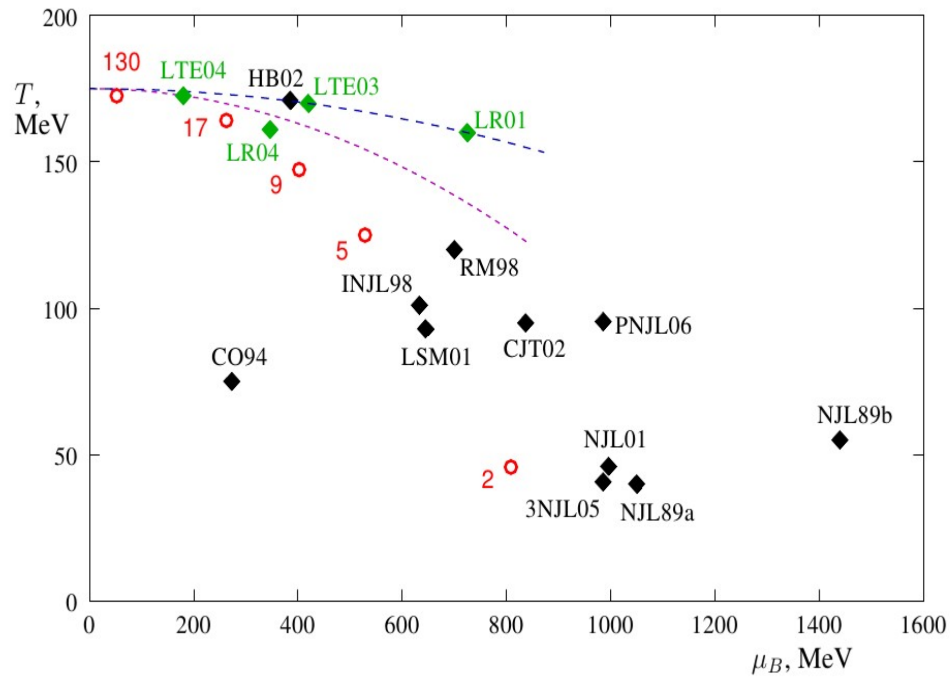

Theoretical predictions

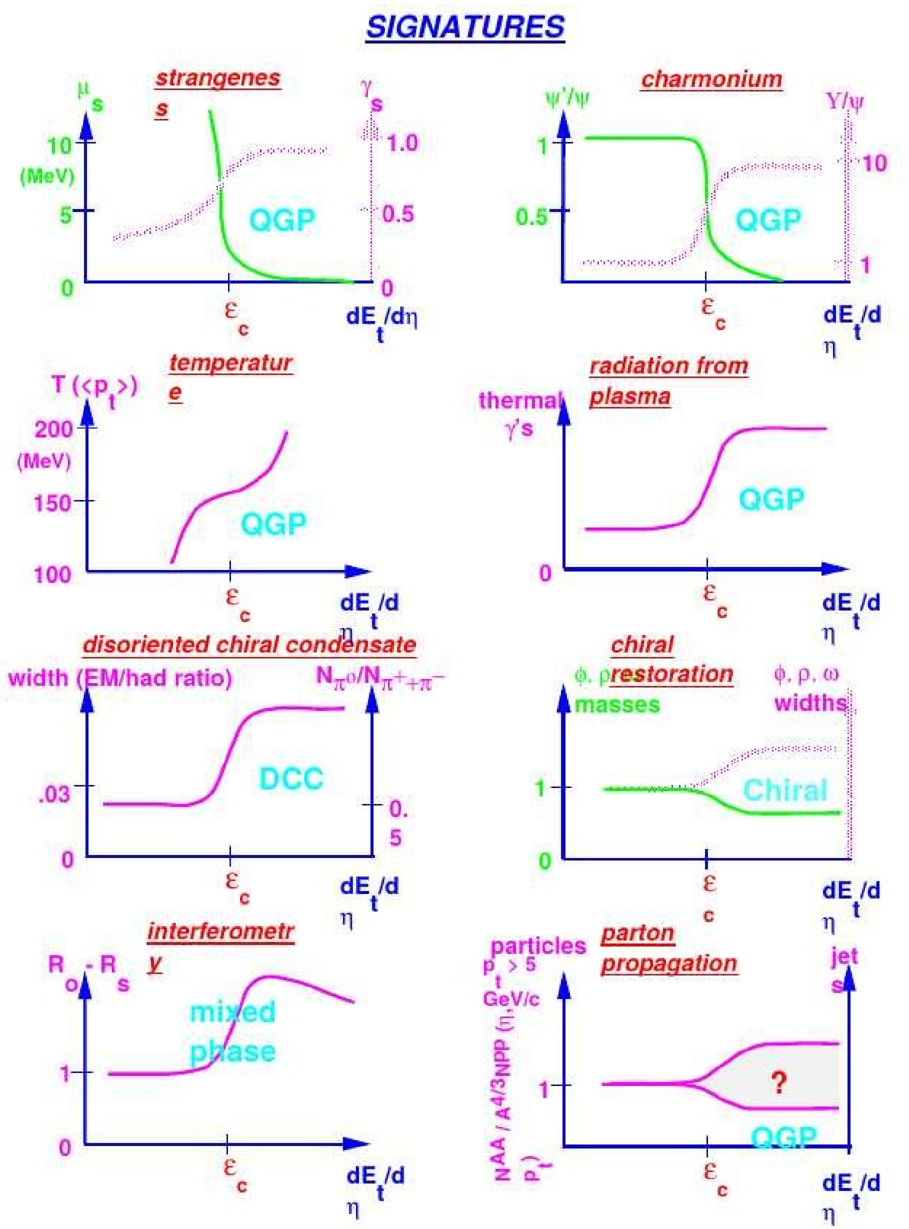

The Search for the Quark-Gluon Plasma

arXiv:hep-ph/9602235
John W. Harris, Berndt Müller

Signatures of quark-gluon plasma formation and the chiral phase transition. The expected behavior of the various signatures is plotted as a function of the measured transverse energy, which is a measure of the energy density, in the region around the critical energy density ε_c of the transition.

When two curves are drawn, the hatched curve corresponds to the variable described by the hatched ordinate on the right.

Studying the Phase Diagram of QCD Matter at RHIC

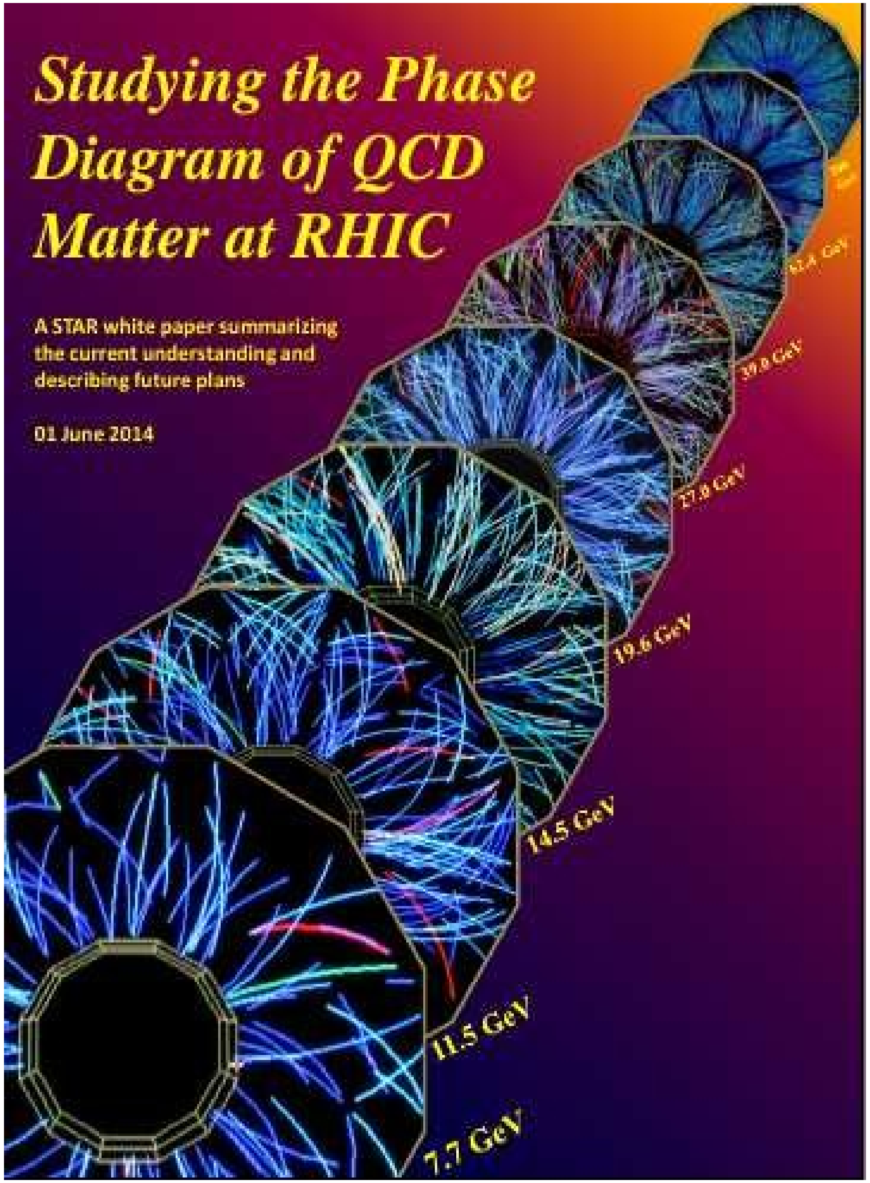

Contents

1 Introduction **3**

2 Review of BES-I Results and Theory Status **5**
- 2.1 Region of the Phase Diagram Accessed in BES-I . . . 5
- 2.2 Search for the Critical Point . . . 8
- 2.3 Search for the First-order Phase Transition . . . 10
  - 2.3.1 Directed Flow (v_1) . . . 10
  - 2.3.2 Average Transverse Mass . . . 12
- 2.4 Search for the Threshold of QGP Formation . . . 13
  - 2.4.1 Elliptic Flow . . . 13
  - 2.4.2 Nuclear Modification Factor . . . 18
  - 2.4.3 Dynamical Charge Correlations . . . 21
  - 2.4.4 Chiral Transition and Dileptons . . . 24
- 2.5 Summary of BES-I . . . 27

3 Proposal for BES Phase-II **30**
- 3.1 Physics Objectives and Specific Observables . . . 30
  - 3.1.1 R_{CP} of identified hadrons up to p_T = 5 GeV/c . . . 32
  - 3.1.2 The v_2 of ϕ mesons and NCQ scaling for indentified particles . . . 33
  - 3.1.3 Three-particle correlators related to CME/LPV . . . 34
  - 3.1.4 The centrality dependence of the slope of $v_1(y)$ around midrapidity . . . 36
  - 3.1.5 Proton-pair correlations . . . 38
  - 3.1.6 Improved $\kappa\sigma^2$ for net-protons . . . 40
  - 3.1.7 Dilepton production . . . 41
- 3.2 Beam request . . . 43
- 3.3 The Fixed-Target Program . . . 45
- 3.4 The Importance of p+p and p+A Systems . . . 45
- 3.5 Collider Performance . . . 47
- 3.6 Detector Upgrades . . . 47
  - 3.6.1 *iTPC* . . . 48
  - 3.6.2 *EPD* . . . 49

4 Summary **50**

STAR BES program

I

$\sqrt{s_{NN}}$ (GeV)	μ_B (MeV)	MinBias Events (10^6)	Time (weeks)	Year
7.7	420	4.3	4	2010
11.5	315	11.7	2	2010
14.5	**260**	**24.0**	**3**	**2014**
19.6	205	35.8	1.5	2011
27.0	155	70.4	1	2011
39.0	115	130.4	2	2010
62.4	70	67.3	1.5	2010

II

$\sqrt{s_{NN}}$ (GeV)	μ_B (MeV)	Needed Events (10^6)
7.7	420	100
9.1	370	160
11.5	315	230
14.5	**260**	**300**
19.6	205	400

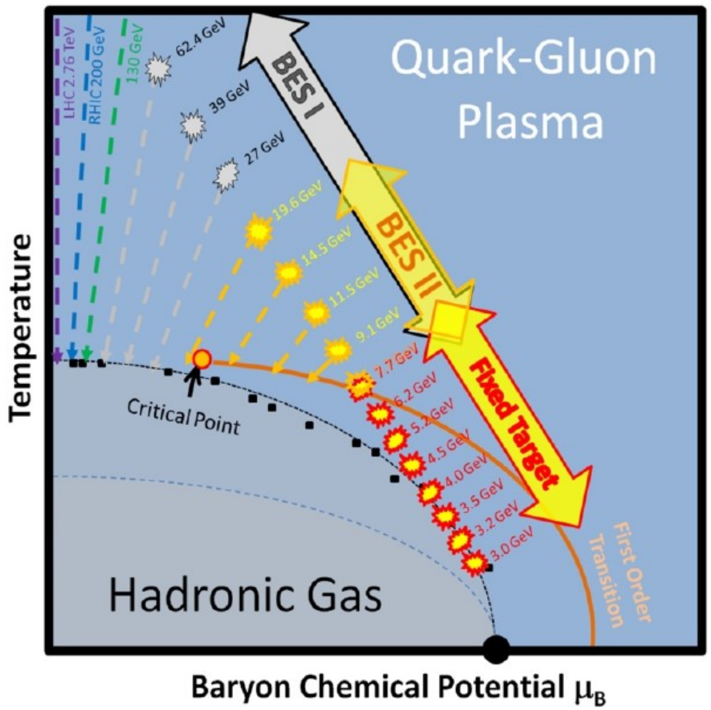

Year	System and Energy	Physics/Observables	Upgrade
2017	• p+p @ 500 GeV • Au+Au @ 62.4 GeV	• Spin sign change diffractive • Jets	FMS post-shower, EPD (1/8th), eTOF prototype
2018	• Zr+Zr, Ru+Ru @ 200 GeV • Au+Au @ 27 GeV	• CME, di-leptons • CVE	Full EPD? eTOF prototype
2019	Au+Au @ 14.5-20 GeV + fixed target	• QCD critical point • Phase transition • CME, CVE,…	Full iTPC, eTOF, and EPD
2020	Au+Au @ 7-11 GeV + fixed target	• QCD critical point • Phase transition • CME, CVE,…	
2020+	• Au+Au @ 200 GeV • p+A/p+p @ 200 GeV	• Unbiased jets, open beauty • PID FF, Drell-Yan, longitudinal correlations	• HFT+ • FCS, FTS

STAR BES: net protons

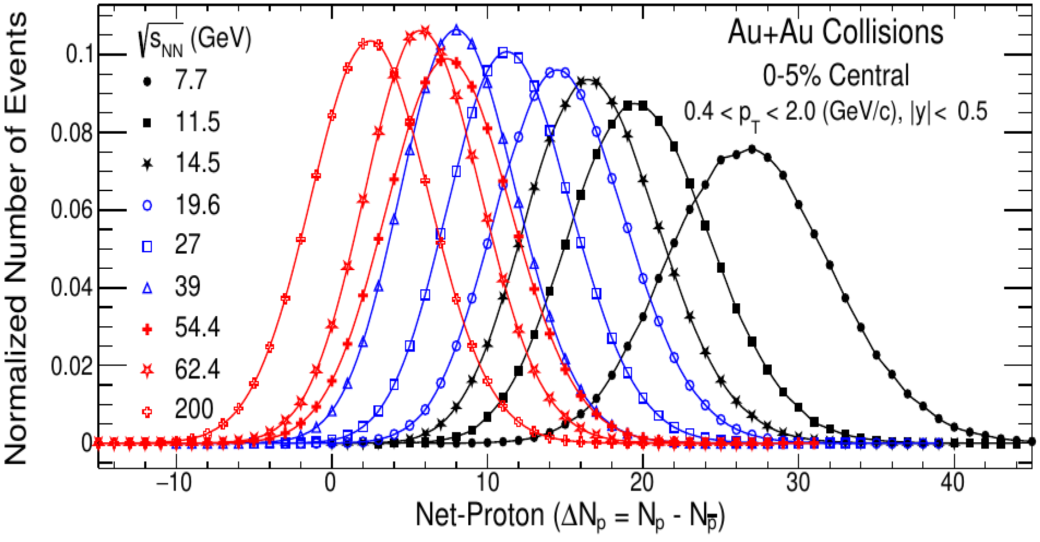

EbyE net-proton number distributions normalized to the total number of events for 0-5% central Au+Au at each $\sqrt{s_{NN}}$

Variation of net-proton cumulants (C_n) as a function of $\sqrt{s_{NN}}$ for central and peripheral Au+Au collisions

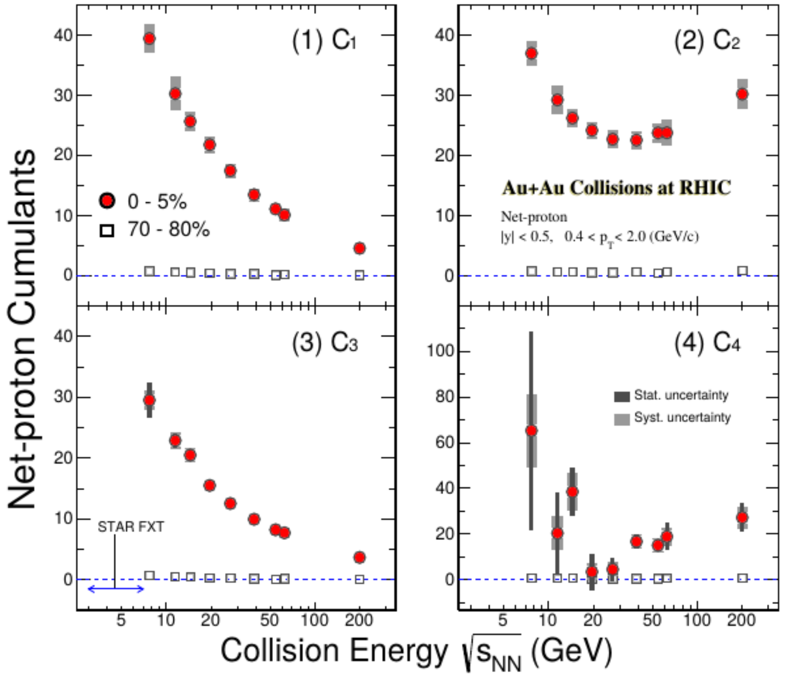

$C_1 = M$, $C_2 = \sigma^2$, $C_3 = S\sigma^3$ and $C_4 = K\sigma^4$

STAR BES: net protons high moments

Ratios of cumulants are related to the ratio of baryon-number susceptibilities:

$(\chi_n^B = \frac{d^n P}{d\mu_B^n}$, where n is the order and P is the pressure of the system at a given T and μ_B .

QCD models : $C_3/C_2 = S\sigma = (\chi_3^B/T)/(\chi_2^B/T^2)$ and $C_4/C_2 = \kappa\sigma^2 = (\chi_4^B)/(\chi_2^B/T^2)$.

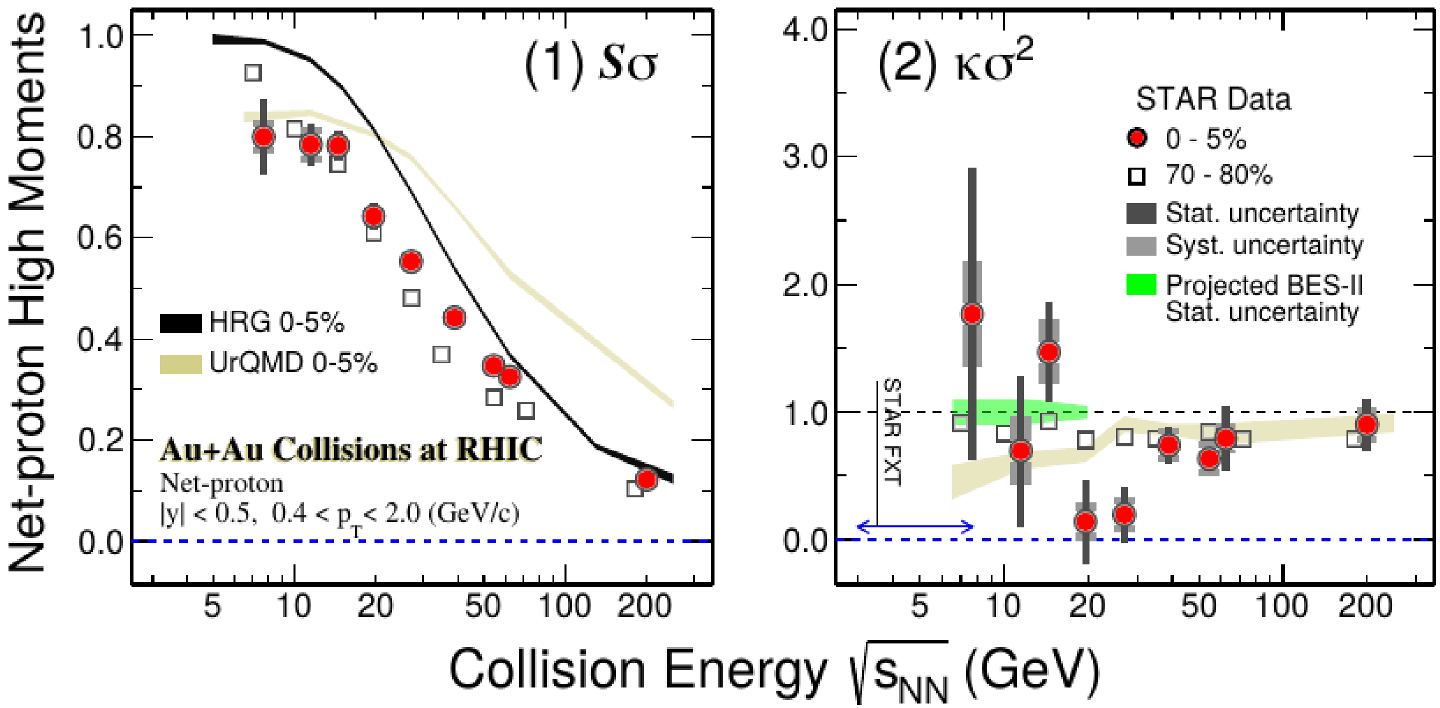

QCD-based calculations predict the net-baryon number distributions to be non-Gaussian and susceptibilities to diverge, causing moments, especially higher-order quantities like $\kappa\sigma^2$, to have non-monotonic variation as a function of $\sqrt{s_{NN}}$

STAR BES: direct flows

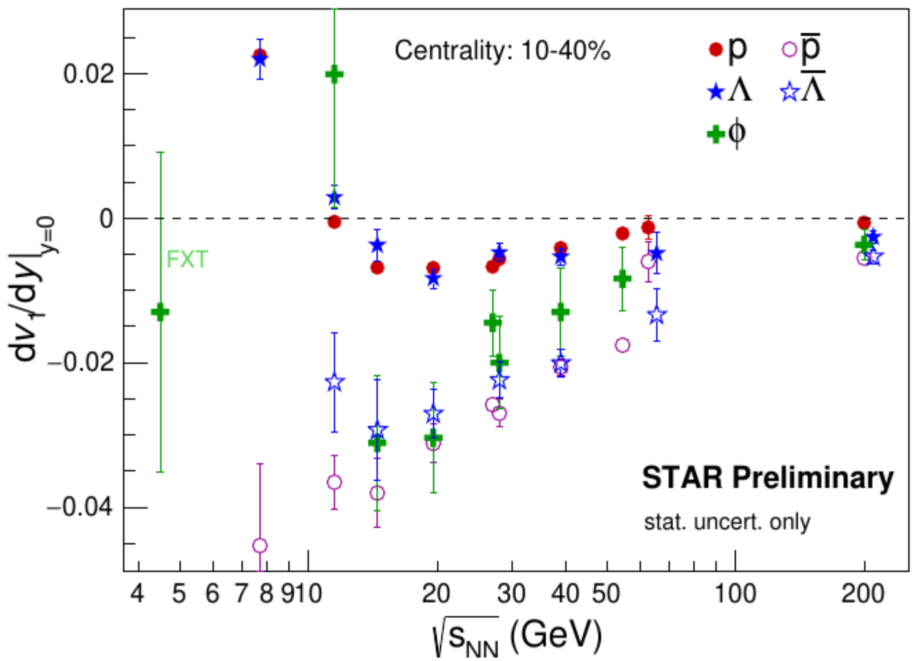

Slope change of baryons (proton and Λ) from positive to negative with increase in energy around $\sqrt{s_{NN}}$ = 14.5 GeV, which might be an indication of softening of EoS around the same energy as predicted by various hydrodynamics and a transport models. In some hydrodynamic calculation, a minimum in directed flow has been proposed as a signature of a first order phase transition between hadronic matter and Quark-Gluon Plasma phases.

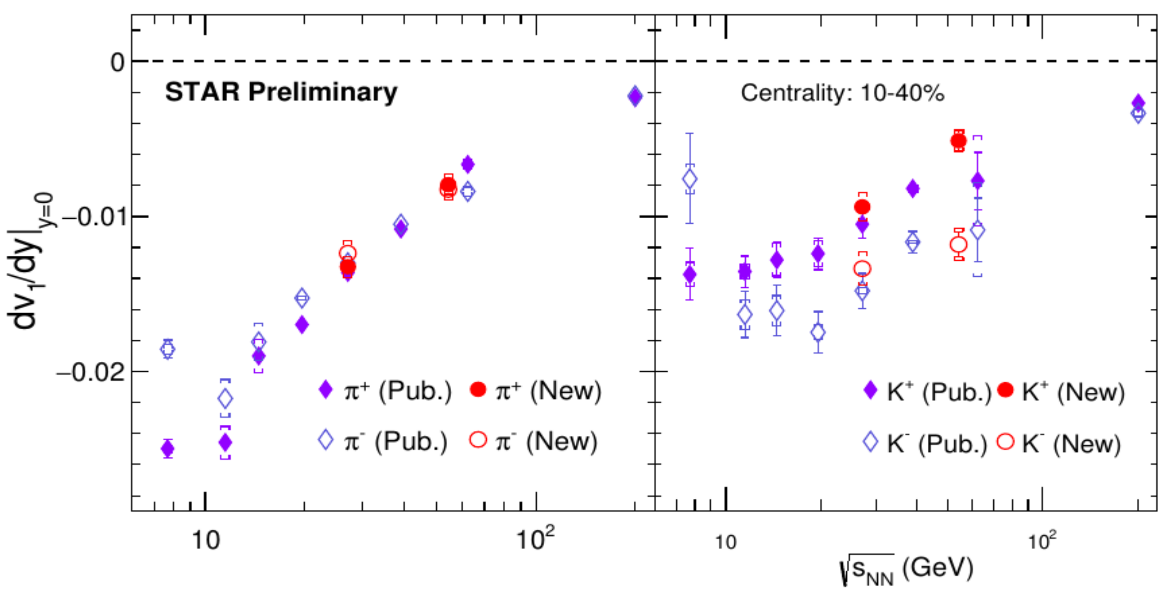

nuclei formation mechanism

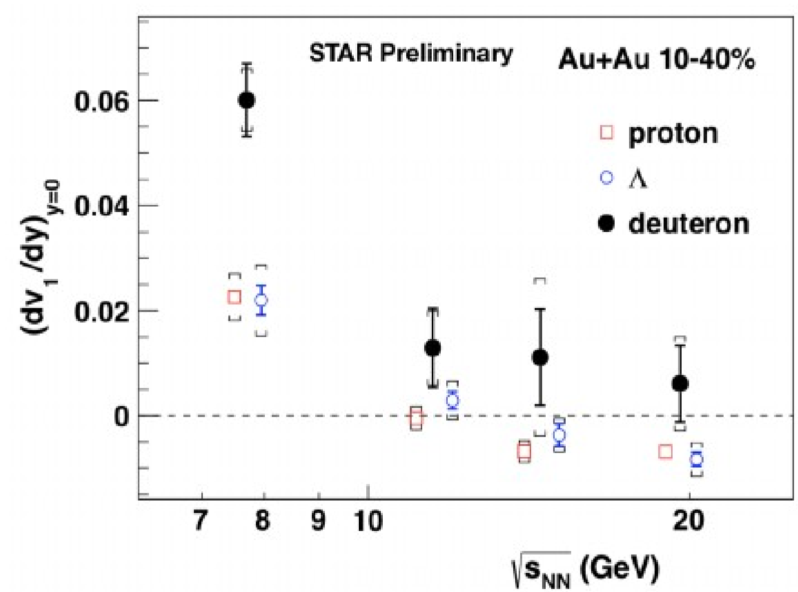

STAR BES: N_{CQ} scaling

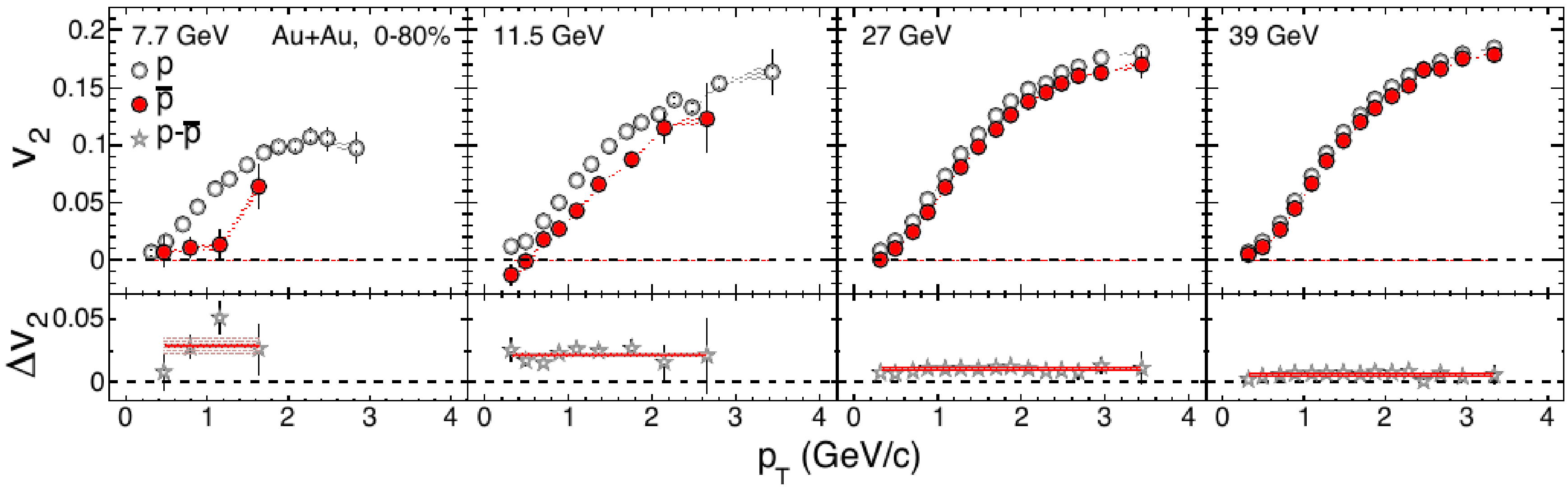

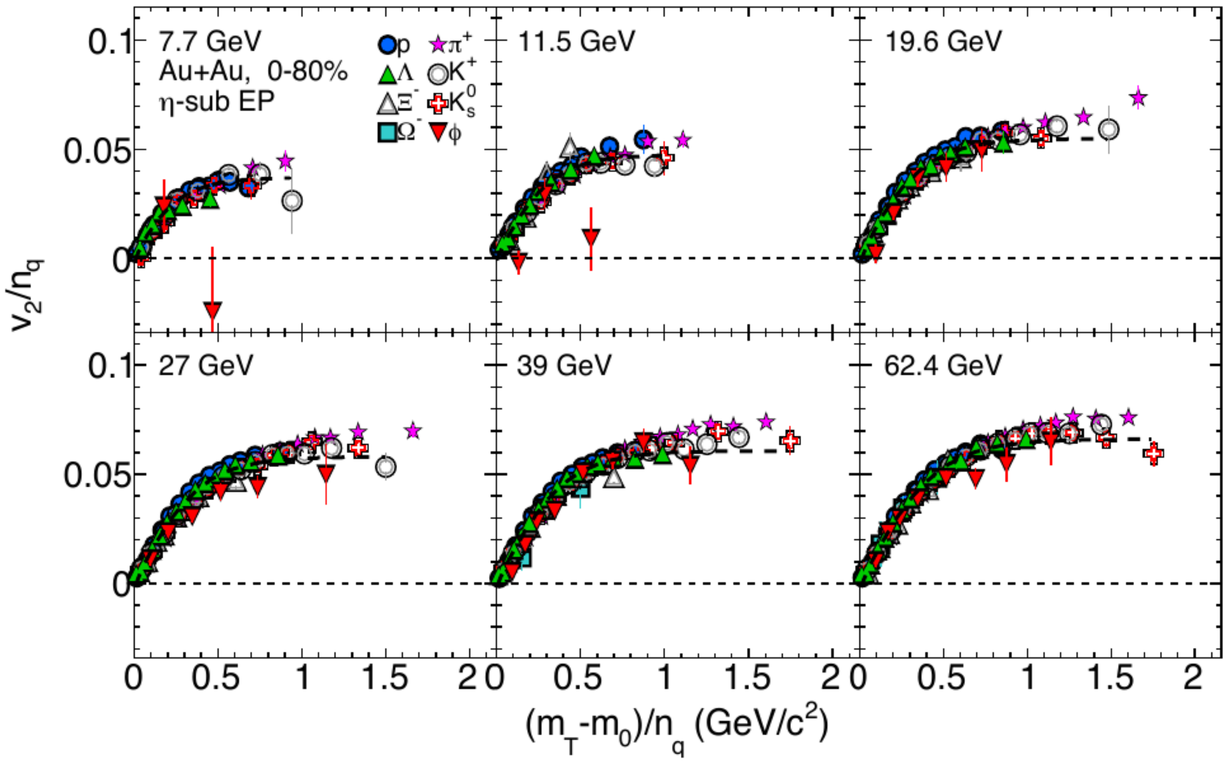

Difference increases substantially with decreasing beam energy.

Phys. Rev. C 93 (2016) 014907

The NCQ scaled elliptic flow v_2 /nq vs $(m_t$-m0)/nq for 0-80% central Au+Au collisions selected particles.

different behavior of v_2 at 7.7 GeV and 11.5 GeV for φ

Elliptic flow fluctuations

Beam energy dependence of Relative elliptic flow fluctuations

Star data: L. Adamczyk et al. (STAR Collaboration). Phys. Rev. C 86, 054908 (2012)
Analysis of the model data: Vinh Ba Luong, Dim Idrisov (MEPhI)

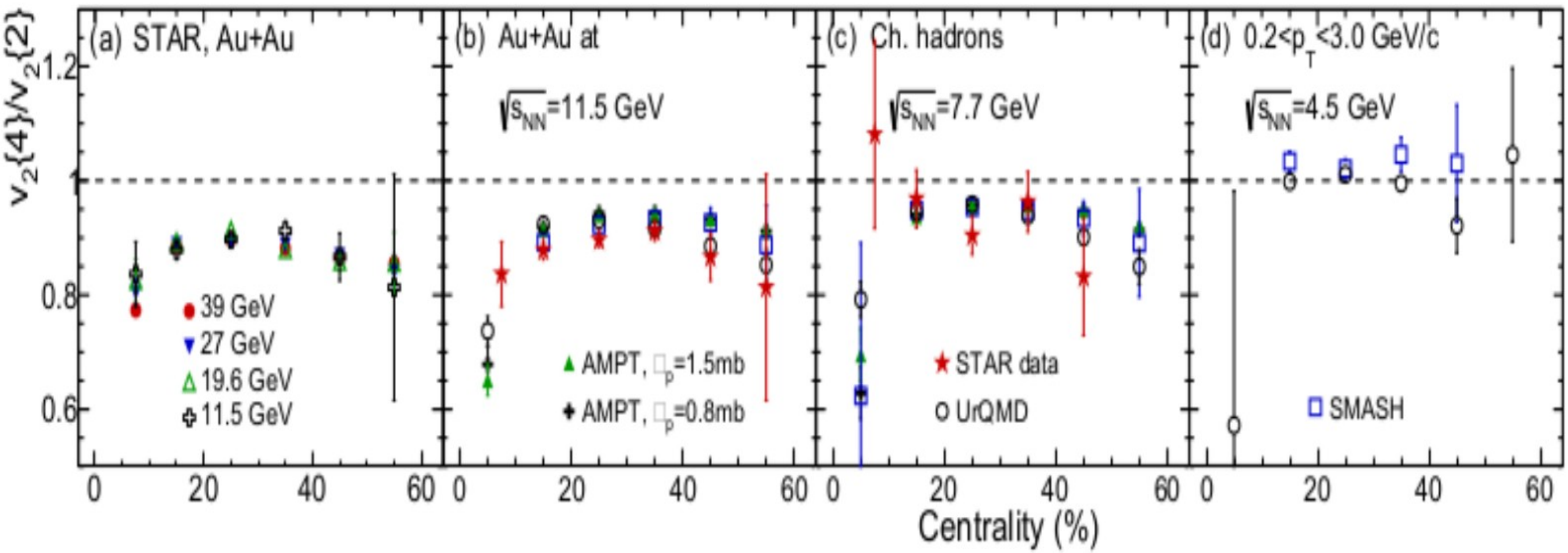

- Relative v_2 fluctuations ($v_2\{4\}/v_2\{2\}$) observed by STAR experiment can be reproduced both in the string/cascade models (UrQMD, SMASH) and hybrid model (AMPT with string melting)
- Dominant source of v_2 fluctuations: participant eccentricity fluctuations in the initial geometry

STAR BES: femtoscopy

HADES, E895, STAR, E866

$\pi^-\pi^-$ pairs created from tracks with transverse momentum $0.1 < p_T < 0.3$ GeV/c
events centrality 0-10%
transverse momentum of the pairs $0.15 < k_T < 0.6$ GeV/c

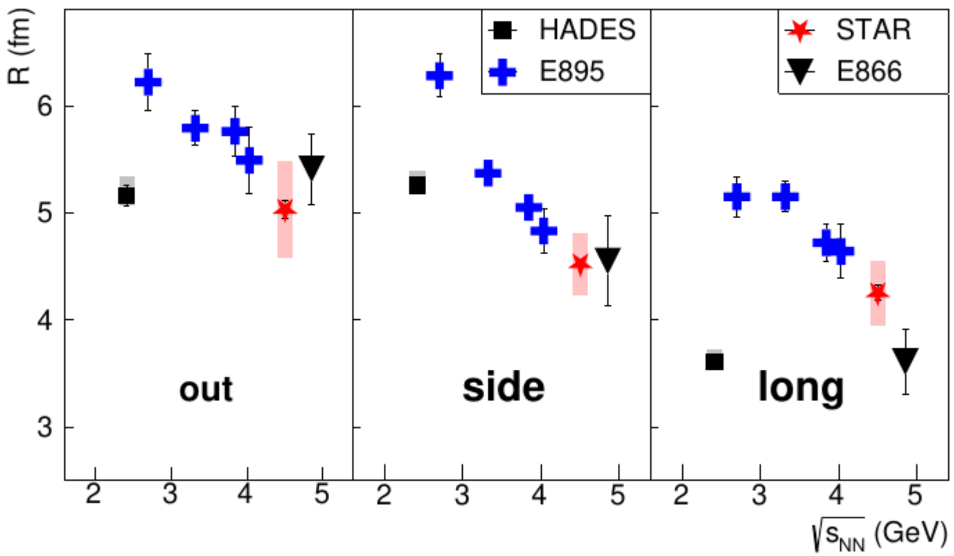

Excitation function of R_{out}, R_{side} and R_{long}

STAR - systematic (red boxes)
and statistical errors (black lines)
errors for E895 and E866 are statistical only.

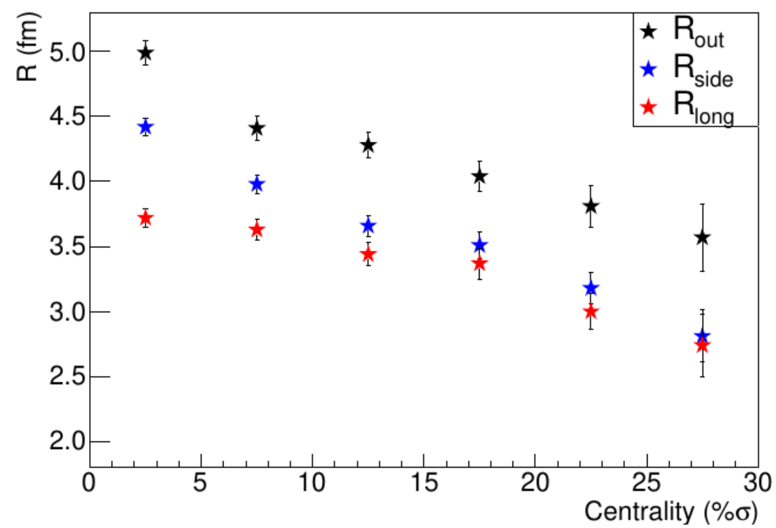

The centrality dependence of R_{out} , R_{side} , and R_{long} .
Errors are statistical only.
$\pi^+\pi^+$ and $\pi^-\pi^-$ pairs in the
momentum range $0.15 < p_T < 0.8$ GeV/c

STAR BES results

net particles flows

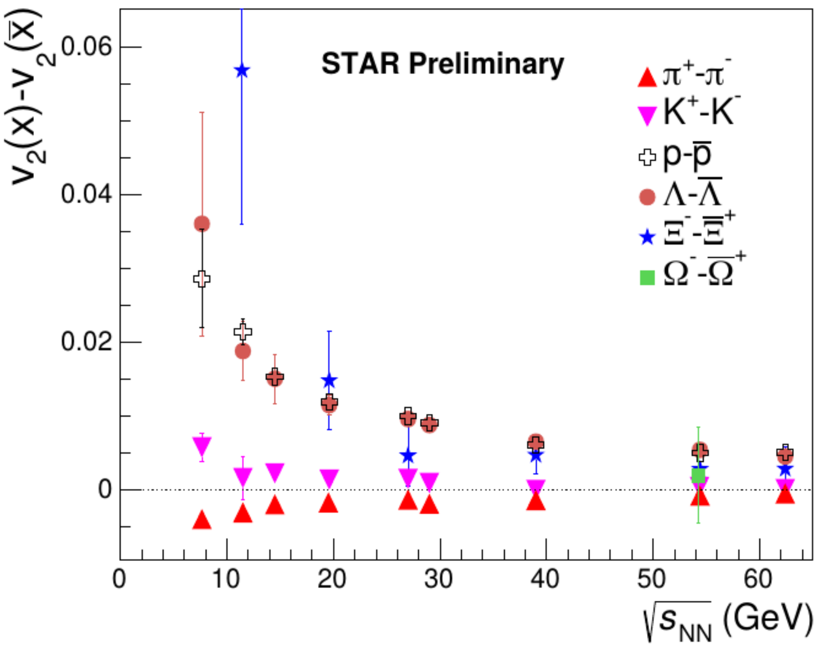

v_2 difference between the particle and anti-particle as a function of beam energy for minimum bias Au+Au collision

high p_T suppression

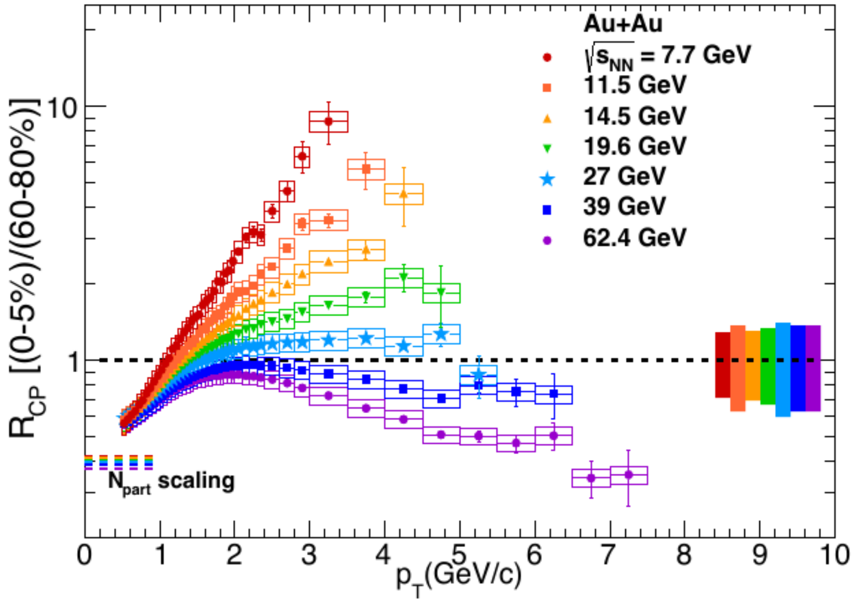

Disappearance of the standard QGP signature is the strong suppression of high p_T charge particles (~ jet quenching), as indicated by binary scaled yields, which is no longer present in the collisions of the BES lower energies for any centrality.

Nuclotron based Ion Collider fAcility

Beams – p,d(h)..$^{197}Au^{79+}$

Collision energy $\sqrt{s}$= **4-11** GeV/u (Au), **12-27** (p)

Beam energy (fixed target) - **1-6** GeV/u

Luminosity: 10^{27} $cm^{-2}s^{-1}$(Au), 10^{32} (p)

Experiments:

2 Interaction points – **MPD** and SPD

Fixed target experiment **BM@N**

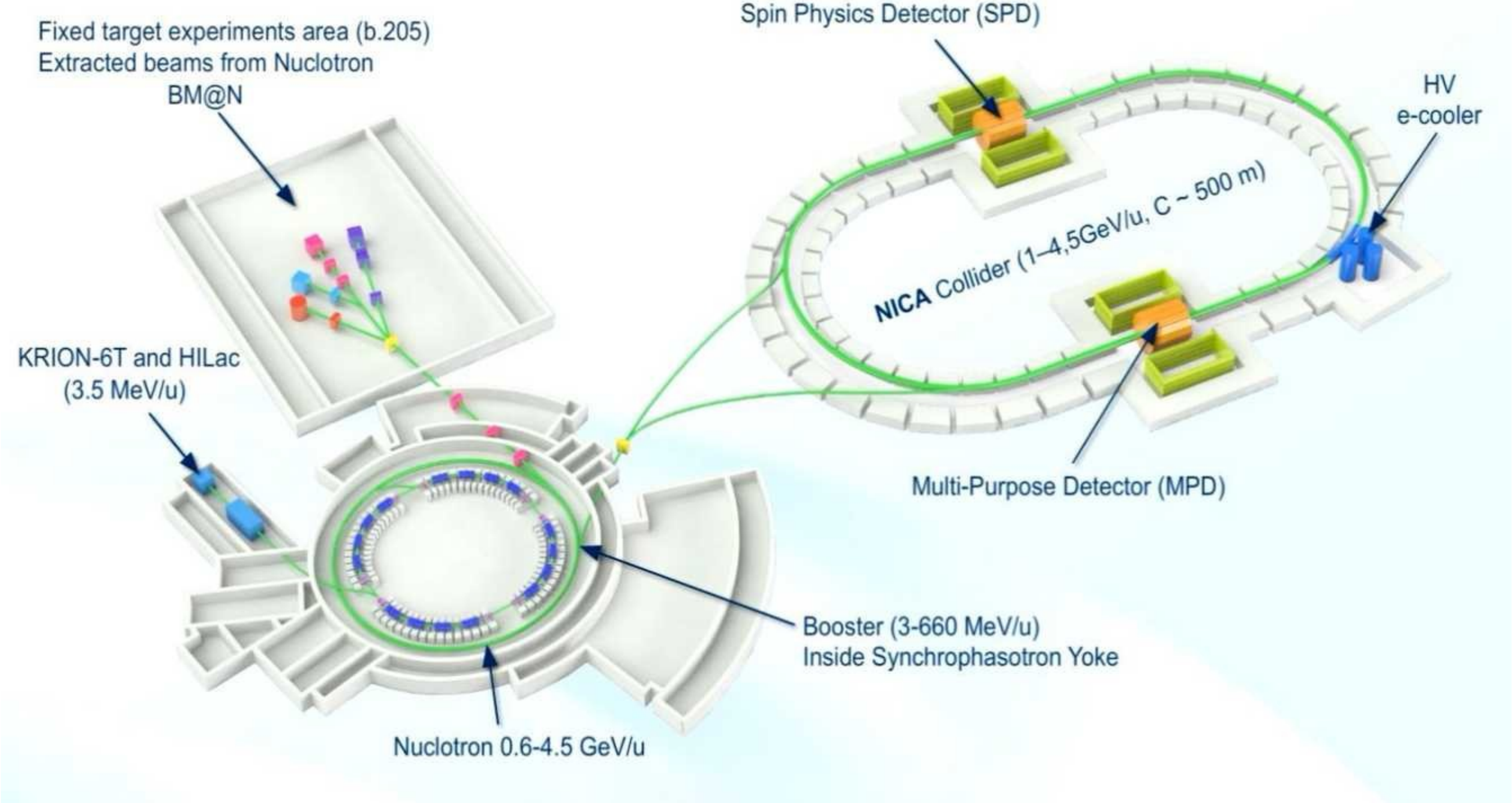

NICA White Paper

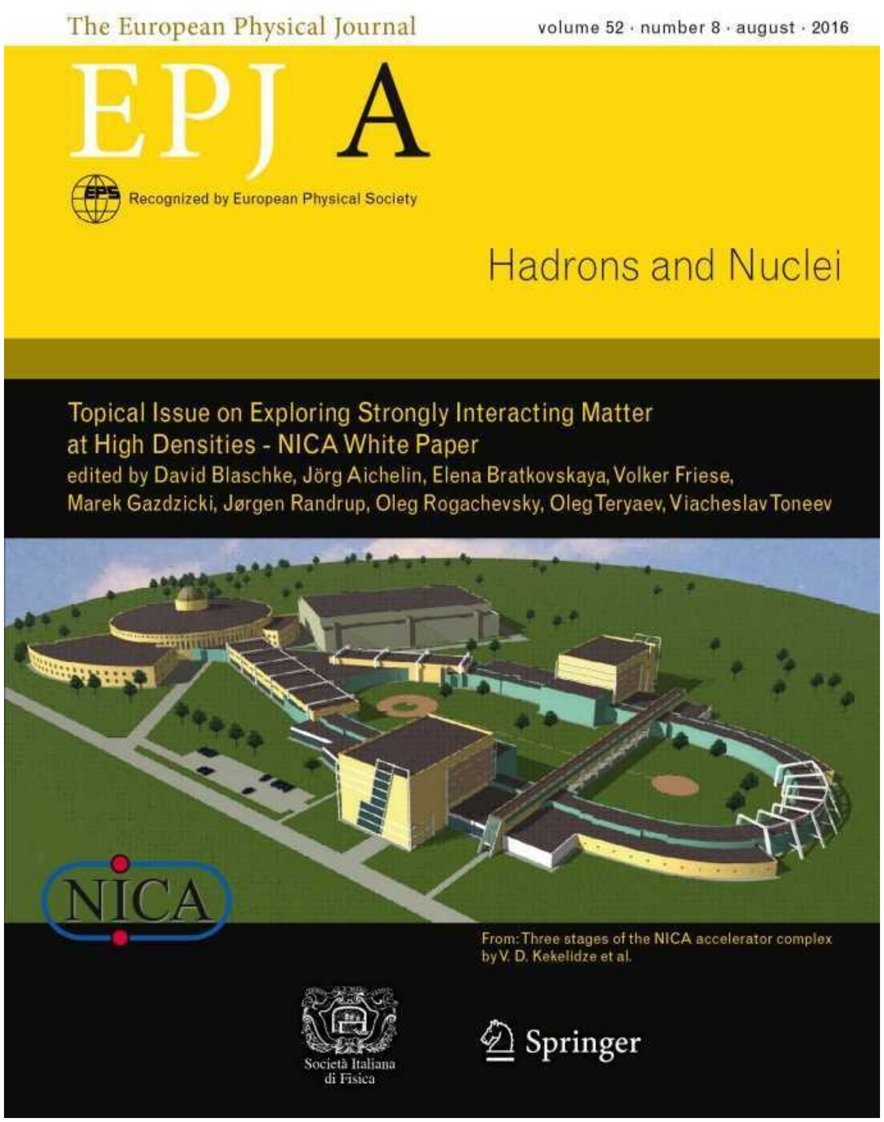

ФИЗИКА ЭЛЕМЕНТАРНЫХ ЧАСТИЦ И АТОМНОГО ЯДРА
2016. Т. 47. ВЫП. 4

FEASIBILITY STUDY OF HEAVY ION PHYSICS PROGRAM AT NICA

P. N. Batyuk [1,], V. D. Kekelidze [1], V. I. Kolesnikov [1],*
O. V. Rogachevsky [1], A. S. Sorin [1,2], V. V. Voronyuk [1]
on behalf of the BM@N and MPD collaborations

[1] Joint Institute for Nuclear Research, Dubna
[2] National Research Nuclear University
"Moscow Engineering Physics Institute" (MEPhI), Moscow

There is strong experimental and theoretical evidence that in collisions of heavy ions at relativistic energies the nuclear matter undergoes a phase transition to the deconfined state — Quark–Gluon Plasma. The caused energy region of such a transition was not found at high energy at SPS and RHIC, and search for this energy is shifted to lower energies, which will be covered by the future NICA (Dubna), FAIR (Darmstadt) facilities and BES II at RHIC. Fixed target and collider experiments at the NICA facility will work in the energy range from a few AGeV up to $\sqrt{s_{NN}} = 11$ GeV and will study the most interesting area on the nuclear matter phase diagram.

The most remarkable results were observed in the study of collective phenomena occurring in the early stage of nuclear collisions. Investigation of the collective flow will provide information on Equation of State (EoS) for nuclear matter. Study of the event-by-event fluctuations and correlations can give us signals of critical behavior of the system. Femtoscopy analysis provides the space-time history of the collisions. Also, it was found that baryon stopping power revealing itself as a "wiggle" in the excitation function of curvature of the (net) proton rapidity spectrum relates to the order of the phase transition.

The available observations of an enhancement of dilepton rates at low invariant masses may serve as a signal of the chiral symmetry restoration in hot and dense matter. Due to this fact, measurements of the dilepton spectra are considered to be an important part of the NICA physics program. The study of strange particles and hypernuclei production gives additional information on the EoS and "strange" axis of the QCD phase diagram.

In this paper a feasibility of the considered investigations is shown by the detailed Monte Carlo simulations applied to the planned experiments (BM@N, MPD) at NICA.

INTRODUCTION	1005
PHYSICS STUDIES FOR THE MPD	1011
PHYSICS STUDIES AT THE NUCLOTORON ENERGIES	1041
THE NICA WHITE PAPER PROPOSALS	1044
SUMMARY	1046
REFERENCES	1046

MPD PWGs

Global observables

- Total event multiplicity
- Total event energy
- Centrality determination
- Total cross-section measurement
- Event plane measurement at all rapidities
- Spectator measurement

Spectra of light flavor and hypernuclei

- Light flavor spectra
- Hyperons and hypernuclei
- Total particle yields and yield ratios
- Kinematic and chemical properties of the event
- Mapping QCD Phase Diag.

Correlations and fluctuations

- Collective flow for hadrons
- Vorticity, Λ polarization
- E-by-E fluctuation of multiplicity, momentum and conserved quantities
- Femtoscopy
- Forward-Backward corr.
- Jet-like correlations

Electromagnetic probes

- Electromagnetic calorimeter meas.
- Photons in ECAL and central barrel
- Low mass dilepton spectra in-medium modification of resonances and intermediate mass region

Heavy flavor

- Study of open charm production
- Charmonium with ECAL and central barrel
- Charmed meson through secondary vertices in ITS and HF electrons
- Explore production at charm threshold

Global observables

Events centrality classes

UrQMD 3.4 AuAu 500k events $\sqrt{s_{NN}}$ = 5, 7.7, 11.5 GeV $|\eta| < 0.5$ $p_T > 0.15$ GeV/c

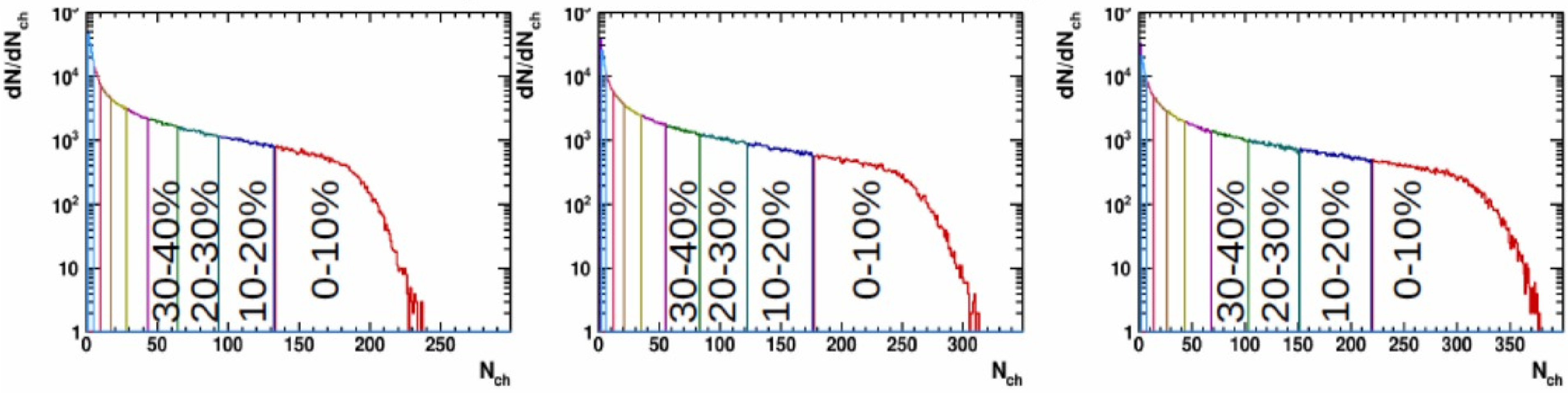

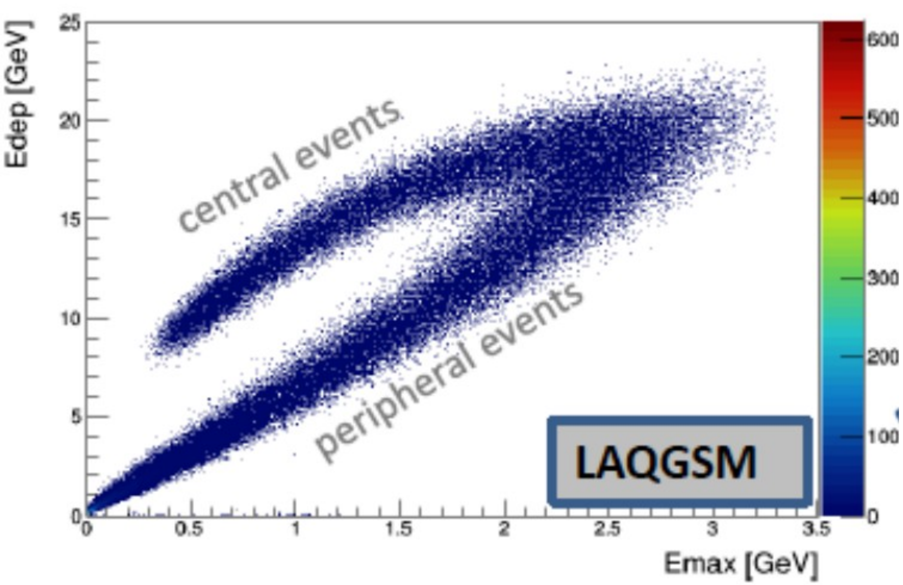

Centrality: 2D-fit of energy distributions (linear approach)

- In this method the space energy distribution in FHCal modules is used.
- The histogram is fitted by a symmetrical cone (linear approximation).
- Weight of each bin is proportional of the energy deposited in corresponding FHCal module.

After linear fit we have:

- E_{fit} is reconstructed energy (volume of cone);
- E_{max} – maximum energy in central bin (in FHCal hole);
- ***Radius*** is defined by the scattering angle of spectators.

Strange and multi-strange baryons

Stage'1 (TPC+TOF): Au+Au @ 11 GeV, PHSD + MPDRoot reco

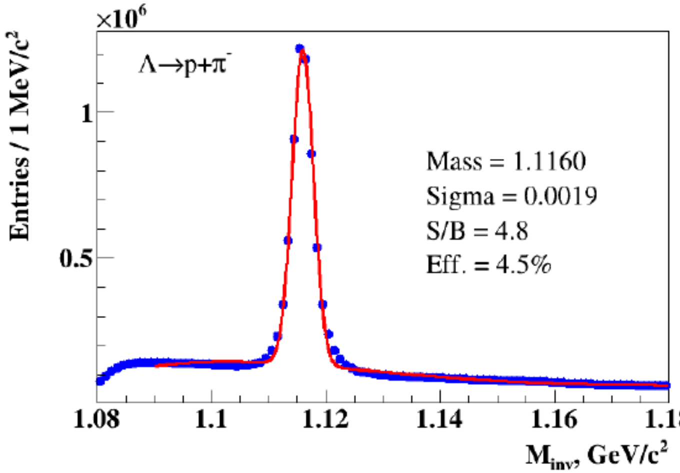

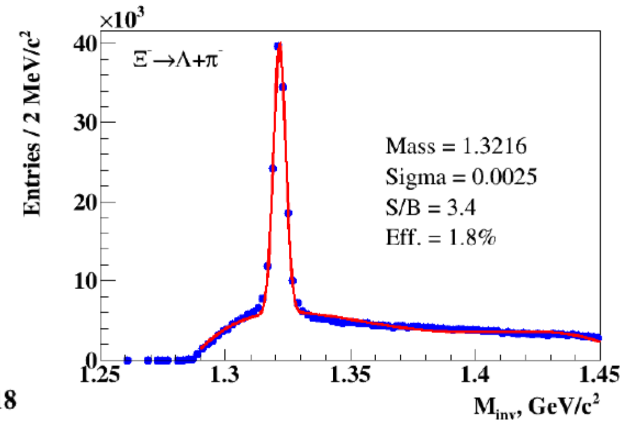

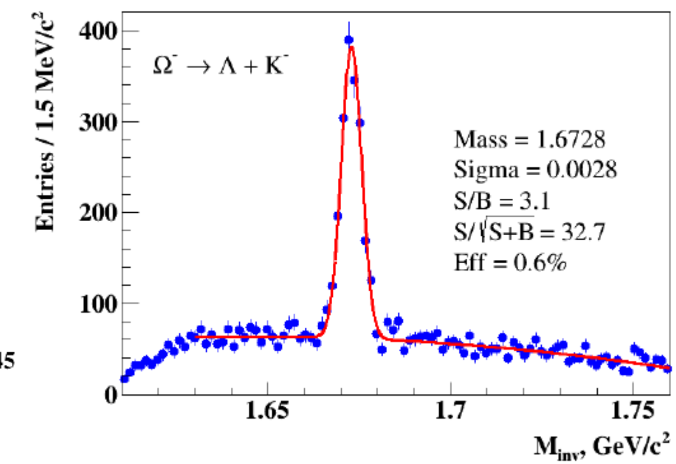

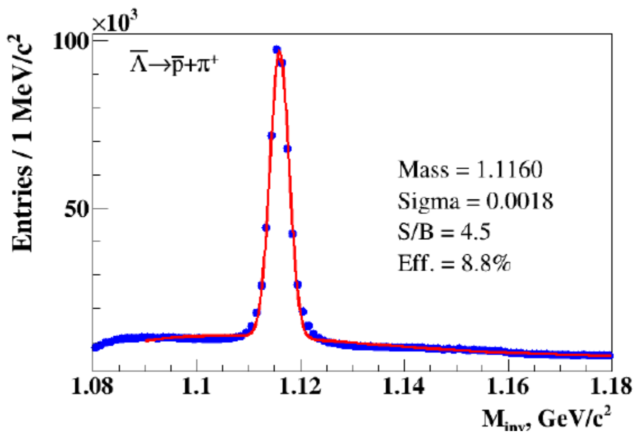

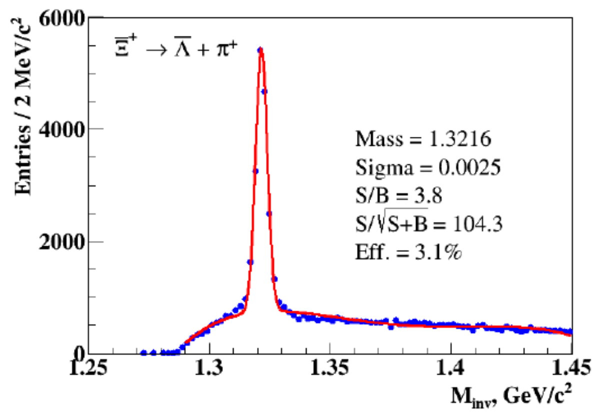

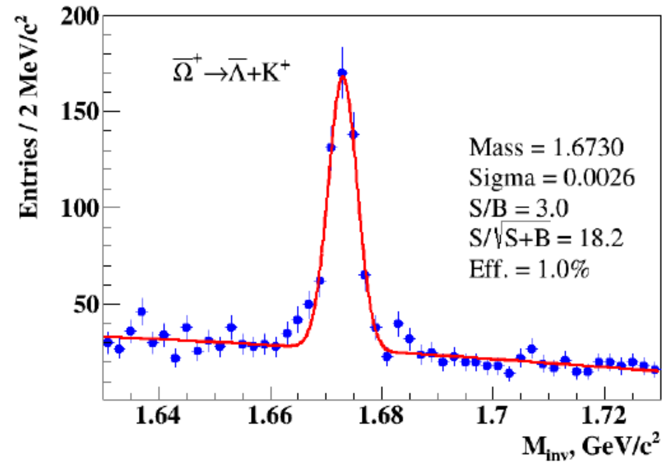

Femtoscopy at MPD

VHLLE model

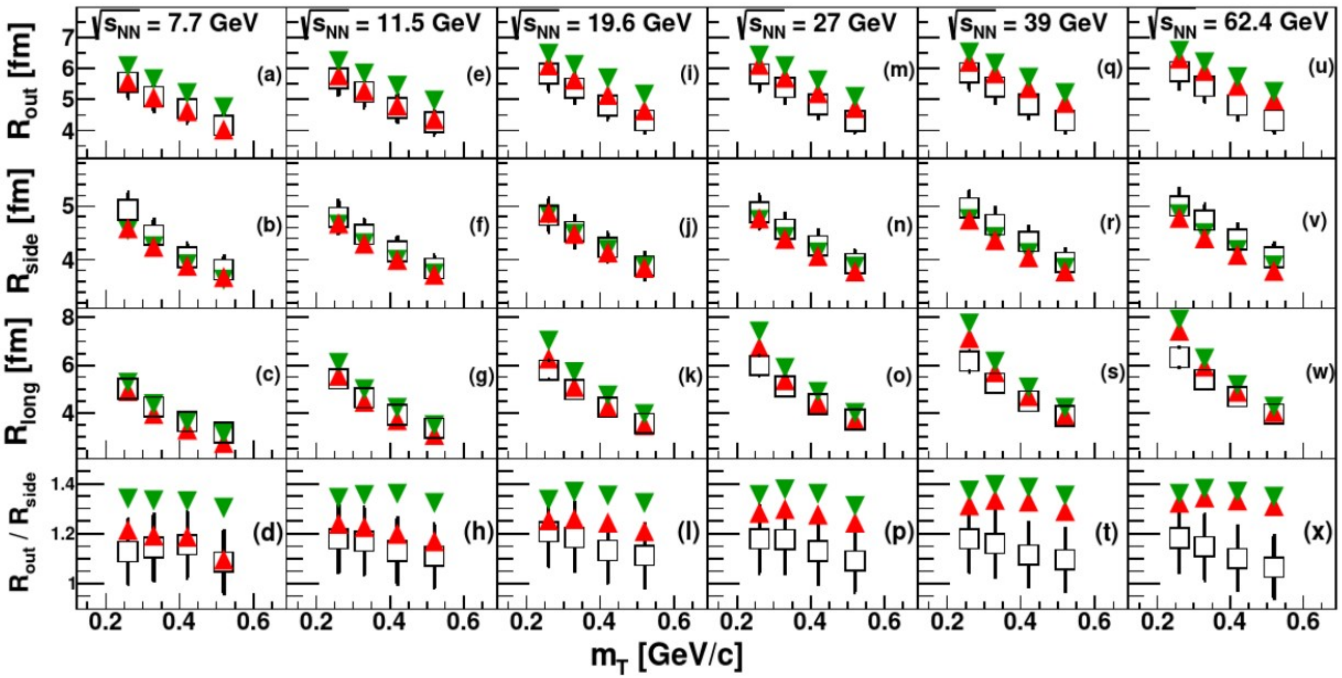

1st order phase transition
Xover phase transition

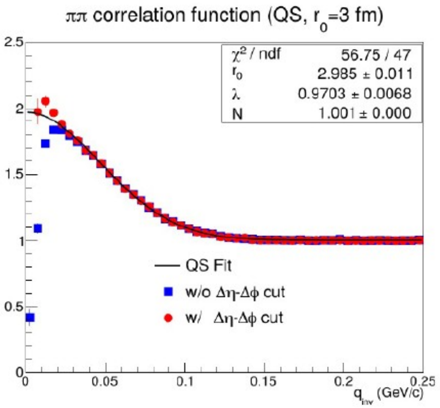

Flows

study of v_2 of pions and protons in MPD

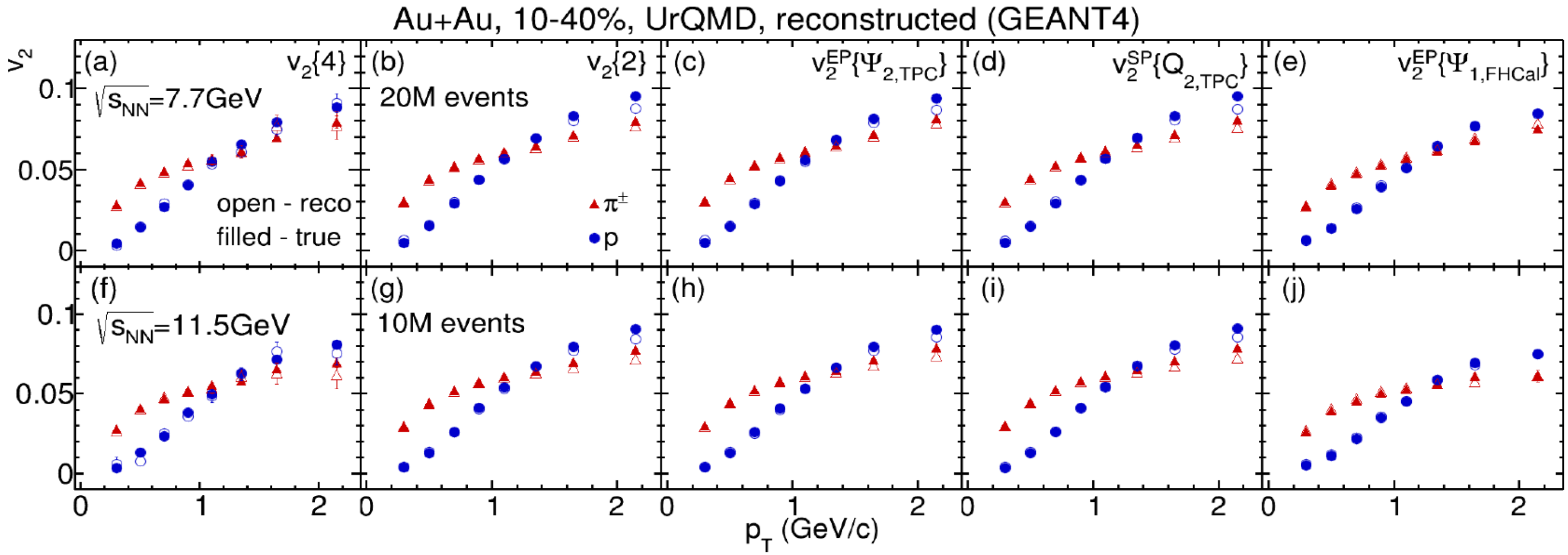

Reconstructed and generated v_2 of pions and protons have a good agreement for all methods

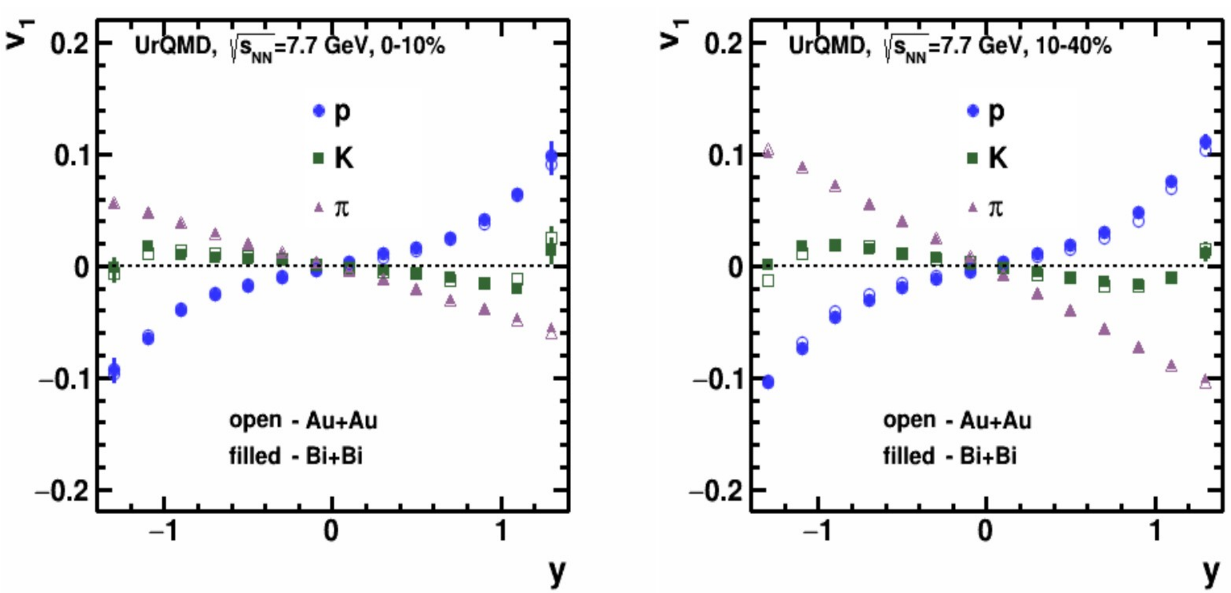

v_1 (y): Bi+Bi vs Au+Au

Small difference for v_1 (y) for particles produced in Au+Au and Bi+Bi collisions.

Electromagnetic probes

Realistic ECAL reconstruction & analysis – large acceptance ECAL with good energy resolution: ideal tool for measurement of neutral mesons in a wide momentum range

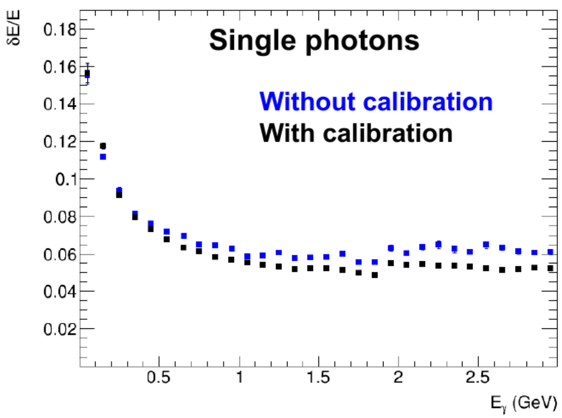

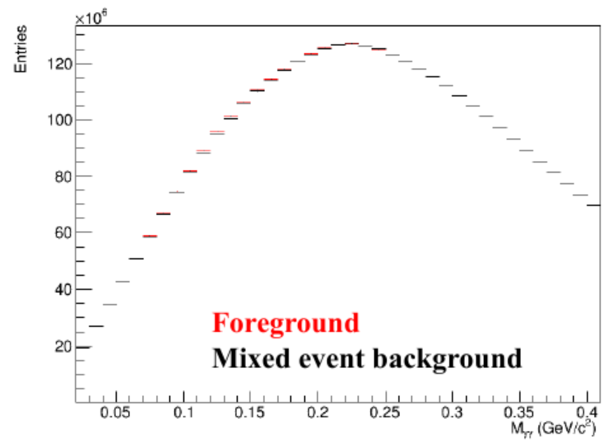

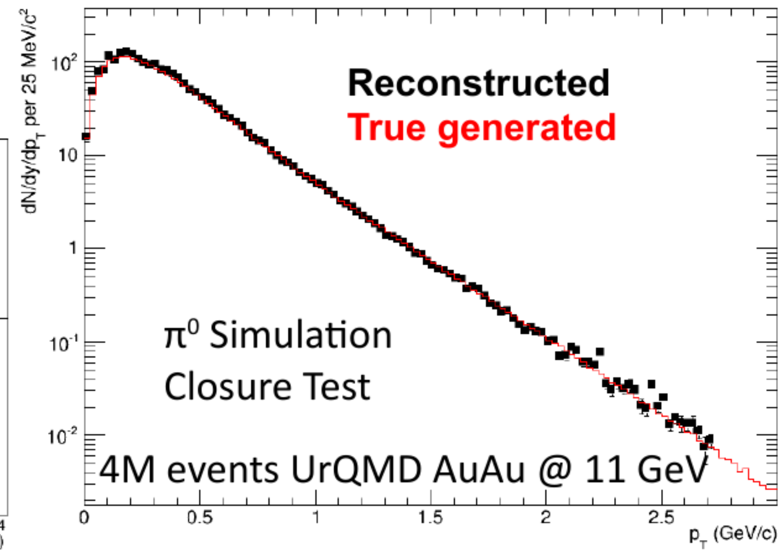

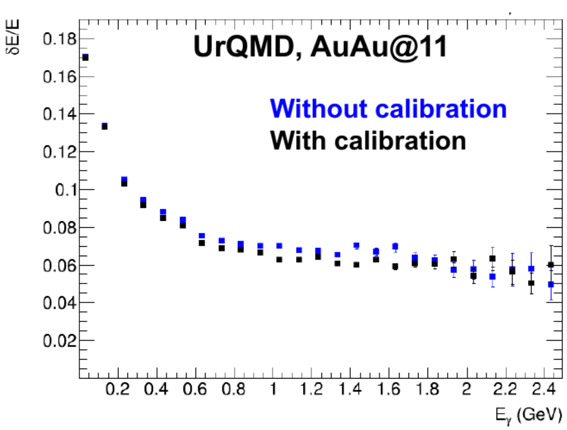

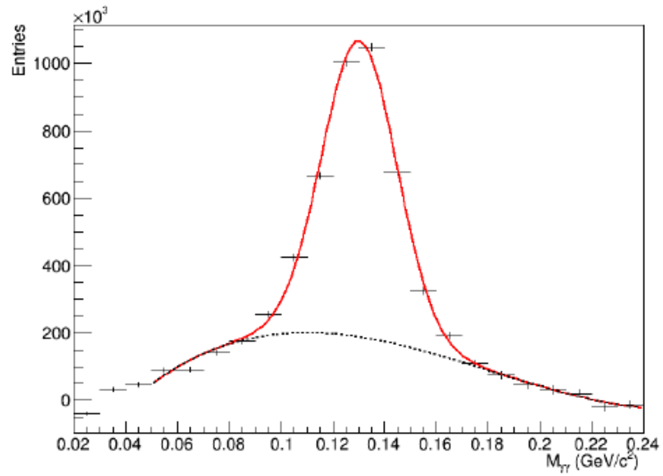

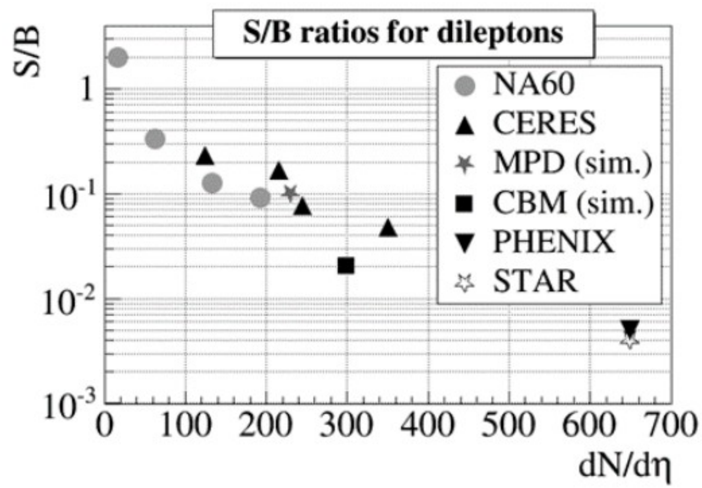

Heavy flavor

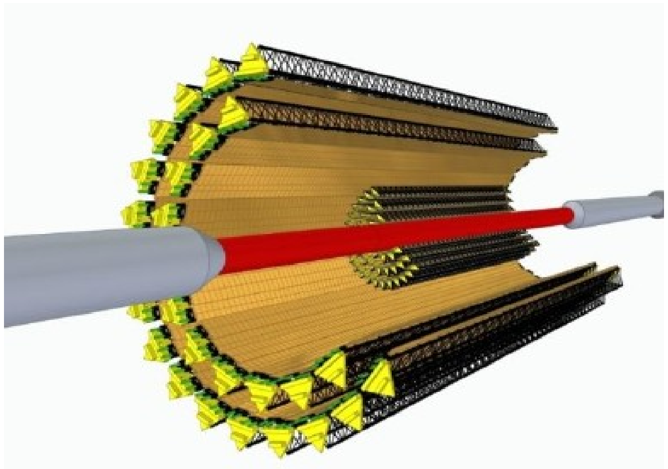

Charmed particle reconstruction in central Au+Au collisions at $\sqrt{S_{NN}}$ = 9 GeV

Particle	Mass [MeV/c^2]	Mean path cτ [mm]	Decay channel	BR
D^+	1869.62±0.20	0.312	$\pi^+ + \pi^+ + K^-$	9.13%
D^0	1864.84±0.17	0.123	$\pi^+ + K^-$	3.89%

$D^0 \rightarrow K^- + \pi^+$

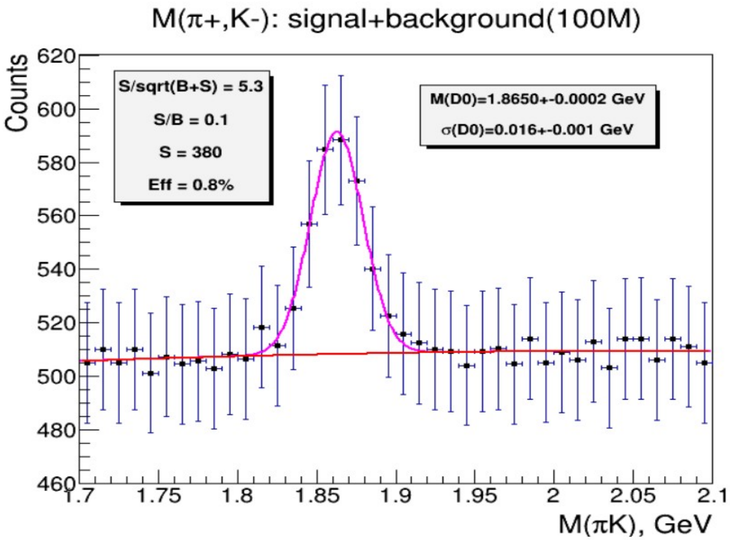

$D^+ \rightarrow K^- + \pi^+ + \pi^+$

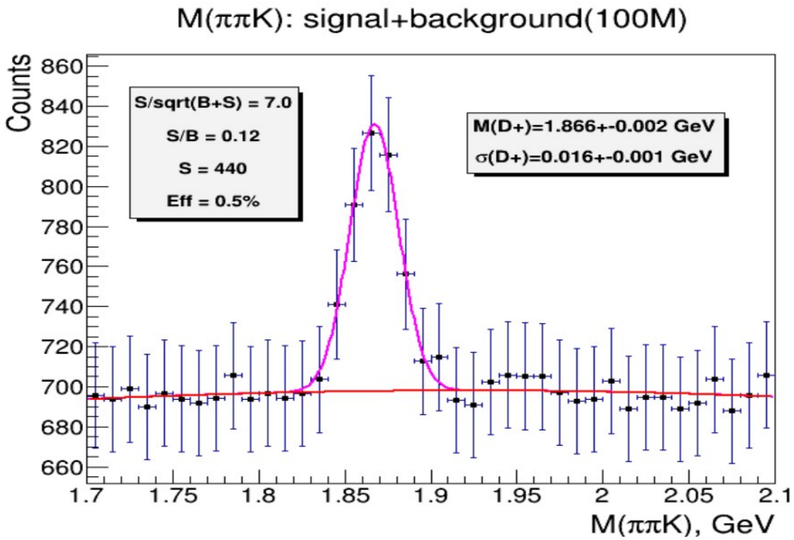

υ_2 at NICA : vHLLE

Elliptic flow at NICA energies: Models vs Data comparison

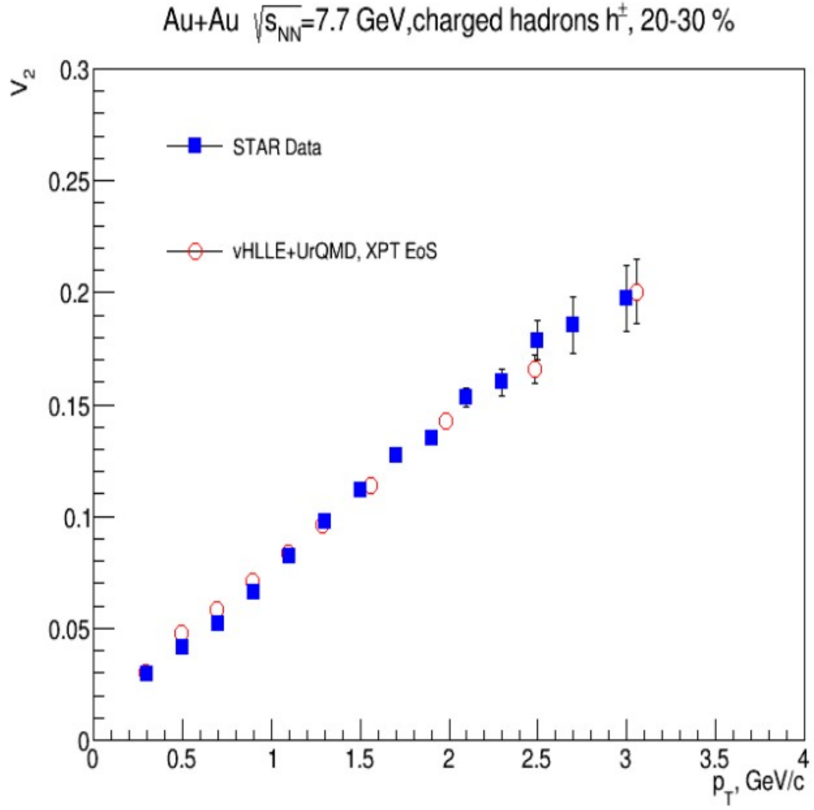

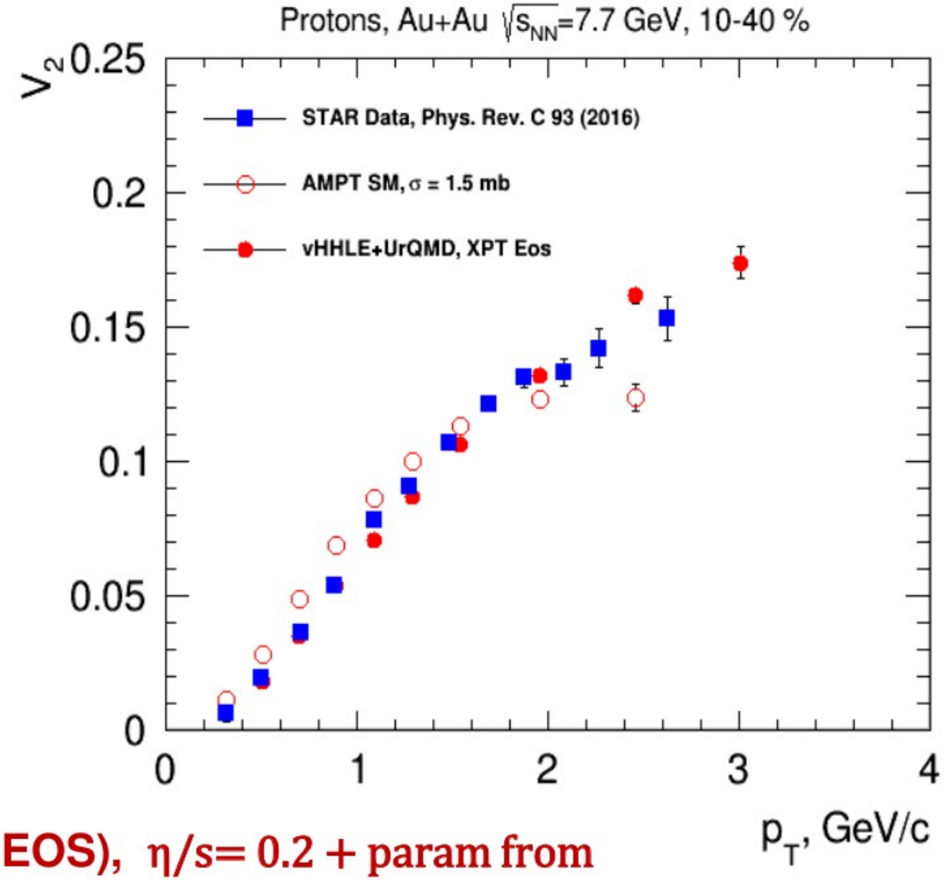

3D hydro model vHHLE + UrQMD (XPT EOS), η/s= 0.2 + param from

Iu.A. Karpenko, P. Huovinen, H. Petersen, M. Bleicher , Phys.Rev. C91 (2015) no.6, 064901

υ_2 at NICA: STAR, UrQMD, SMASH

Elliptic flow at NICA energies: Models vs Data comparison

STAR Data, https://arxiv.org/abs/2007.14005

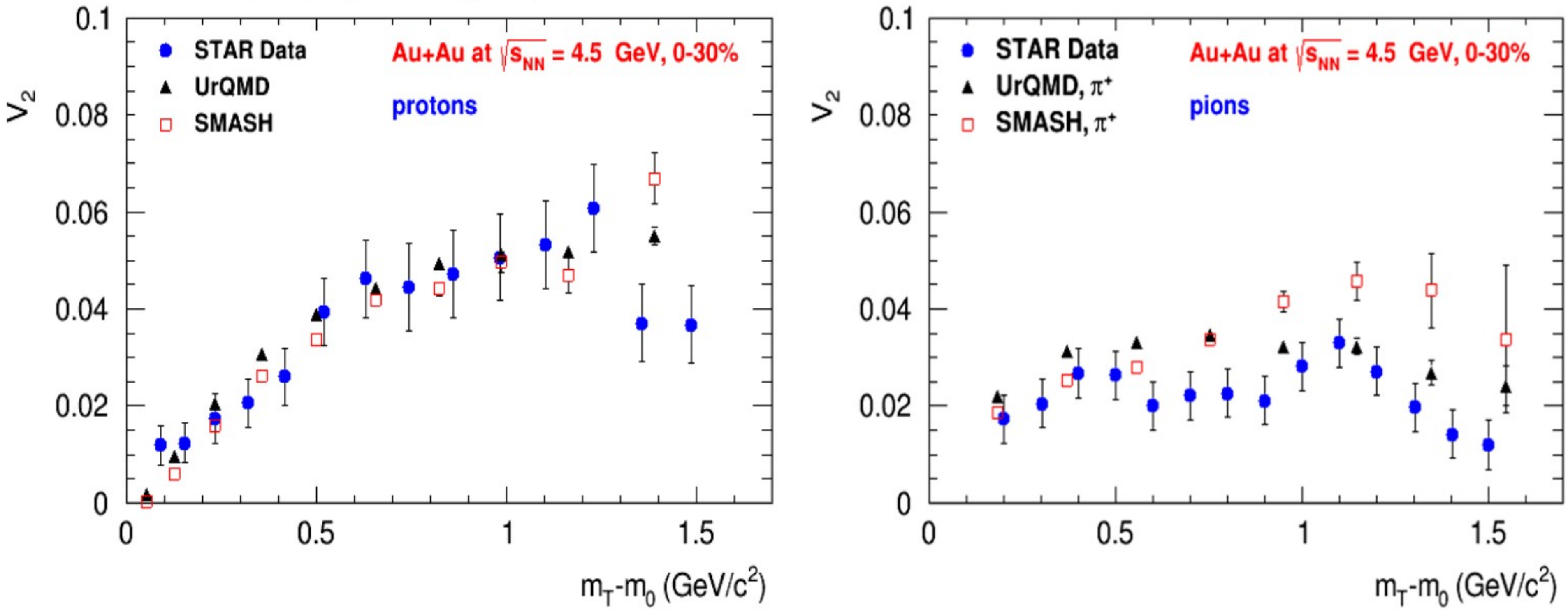

Pure String/Hadronic Cascade models give similar v_2 signal compared to STAR data for Au+Au $\sqrt{s_{NN}}$=4.5 GeV

First physics with MPD experiment at the NICA

First Physics with MPD Experiment at the NICA Accelerator Complex*

Fuqiang Wang, Jiansong Wang, and Xiangrong Zhu
Huzhou University, CHINA

Mei Huang, Minghua Wei, and Kun Xu
Institute of High Energy Physics, CHINA

ChengXin Zhao, Haibo Yang, Yapeng Zhang, Wei Zhou, Yao Wang, Xiaoyang Niu, and Yuezhao Zhang
Institute of Modern Physics of the Chinese Academy of Science, Lanzhou, CHINA

Yugang Ma, Deqing Fang, and Wanbing He
Fudan University, CHINA

Cunfeng Feng, Jianbin Jiao, Qinghua Xu, Chi Yang, and Dong Liu
Shandong University, CHINA

Shengqin Feng, Kejun Wu, and Shuang Li
Three Gorges University, CHINA

Yi Wang, Zhigang Xiao, Xianglei Zhu, Zhi Deng, Zhi Zhang, Yan Huang, Chendi Shen, Yulei Li, and Linmao Li
Tsinghua University, Liuqing Building 611, Beijing, 100084, CHINA

Zebo Tang, Wangmei Zha, Ziwei Li, Pengzhong Lu, and Yan WANG
University of Science and Technology of China, Hefei, CHINA

Wojciech Dominik, Izabela Skwira-Chalot, Tomasz Matulewicz, Magdalena Kuich, Krzysztof Piasecki, Skwira-Chalot Izabela, Matulewicz Tomasz, Dominik Wojciech, Kuich Magdalena, and Piasecki Krzysztof
University of Warsaw, POLAND

Botvina Alexander, Golubeva Marina, Guber Fedor, Ivashkin Alexander, Izvestnyy Alexander, Karpushkin Nikolay, Kurepin Alexey, Morozov Sergey, Petukhov Oleg, Alexander Strizhak, and Vadim Volkov
INR RAS, Moscow, RUSSIA

Viacheslav V. Kulikov, Maxim A. Martemianov, Mikhail A. Matsyuk, and Sergey A. Bulychjov
National Research Center "Kurchatov Institute" – Institute of Theoretical and Exprimental Physics, Moscow, 117218 RUSSIA

Aleksandr Klyuev, Alexander Kubankin, Vitaly Dronik, and Kristina Vokhmyanina
Belgorod National Research University, RUSSIA

Tagir Aushev
Moscow Institute of Physics and Technology, RUSSIA

Baranova Natalia, Bogdanova Galina, Boos Edward, Larisa Bravina, Eyyubova Gulnara, Karmanov Dmitry, Kharlamov Petr, Vyacheslav Klyukhin, Kodolova Olga, Korolev Mikhail, Korotkikh Vladimir, Kryukov Alexander, Valentin Kuzmin, Kukulin Vladimir, Lanskoy Dmitry, Lokhtin Igor, Merkin Mikhail, Sergey Petrushanko, Platonova Maria, Lydia Shcheglova, Solomin Anatoly, Tretyakova Tatiana, Volkov Vladimir, Zabrodin Evgeny, Maria Cheremnova, Gleb Romanenko, and Anna Romanova
SINP, Moscow, RUSSIA

Malinina Ludmila
SINP, Moscow, RUSSIA and
Joint Institute for Nuclear Research, Joliot Curie str., 6, Dubna, 141980, RUSSIA

Kankiewicz Pawel, Rybczynski Maciej, Stefanek Grzegorz, and Wlodarczyk Zbigniew
Jan Kochanowski University, POLAND

Mircea Baznat, Dmitri Baznat, and Andrey Khvorostukhin
Inst. of Applied Physics, Chisinev, MOLDOVA

Sergey Kovalenko, Sergey Kuleshov, Lautaro Leon Narvaez Paredes, Rimsky Rojas Cabellero, Elias Felix Rozas Calderon, Pablo Augusto Ulloa Poblete, Nicolas Viaux Maria, and Jilberto Antonio Zamora Saa
U. Tecnica Federico Santa Maria, Valparaiso, CHILE

Feng Liu, Xiangming Sun, and Yaping Wang
Central China Normal University, CHINA

Jiri Kvita, Miroslav Maslan, Libor Nozka, and Tomas Rossler
Palacky U., Olomouc, CZECH Republic

Nelli Pukhaeva, Yuri Kasumov, Antonina Eremina, Anatoly Korsunov, David Kibizov, Zarina Persaeva, and Ramazan Esenov
North Ossetian State University, Vladikavkaz, RUSSIA

Anar Rustamov
Baku State University, AZERBAIJAN and
National Nuclear Research Center, AZERBAIJAN

Ramin Sattarov
National Nuclear Research Center, AZERBAIJAN

Tamar Babutsidze, Giorgi Kachlishvili, Alexander Machavariani, Mikheil Nioradze, Valeri Kikvadze, and Revaz Shanidze
Tbilisi State University, Tbilisi, GEORGIA

Boyana Dabrowska, Petar Dulov, Nikolay Geraksiev, Mariya Ilieva, Dilyana Suvarieva, Vanio Tcholakov, and Lyubka Yordanova
University of Plovdiv, BULGARIA

Hovik Grigorian, Narine Gevorgyan, Alexander Ayriyan, Vahagn Abgaryan, and Arpine Piloyan
A. Alikhanyan National Lab of Armenia, ARMENIA

(Dated: October 26, 2020)

The Nuclotron-based Ion Collider fAcility (NICA) is in construction at the Joint Institute for Nuclear Research (JINR). The accelerator complex will consists of several components, specifically the Nuclotron accelerator, the Booster support accelerator, two ion sources, as well as the NICA collider ring with the corresponding transfer lines from Nuclotron. The expected date of putting the NICA collider ring for commissioning is September of 2022. At the same time the Multi-Purpose Detector (MPD) has been designed to operate at NICA. Components of MPD are currently in production. The assembly of the detector on-site has started on July of 2020, while on November of 2021 the detector setup will start the commisioning, to be ready for datataking on first beam from NICA.

This documents details the preparation schedule for the construction and commisionning of MPD. It presents the plans for the first physics measurements at NICA and puts them into context of existing and planned physics experiments in the area of QCD phase diagram investigation.

CONTENTS

I. The NICA Complex construction schedule and expected initial performance 5

II. Readiness of the MPD experiment 5

A. Technical infrastructure and support systems 5
1. MPD Hall and facilities 5
2. MPD magnet 6
3. MPD mechanical integration and support structure 6
4. Electronics support infrastructure 7

B. Main MPD detector components for Stage 1 7
1. MPD Time Projection Chamber 7
2. MPD Time Of Flight 8

* A report for the NICA Supervisory Board and the JINR Committee of Plenipotentiaries

3. MPD Electromagnetic Calorimeter 9
4. MPD Forward Hadronic Calorimeter 10
5. Fast Forward Detector 11
6. MPD Cosmic Ray Detector 12
7. MiniBEBE detector 13

C. MPD Electronics 14
1. Slow Control System 14
2. Data Acquisition 14

D. Summary timeline of detector readiness 15

III. Triggering and data rate 15

IV. Computing and software requirements 16
A. MPD Software 17
B. Preparation for data taking and analysis 17

V. Physics goals 17

VI. Plans for first-day MPD Physics 20
A. Calibration and alignment 20
1. Tracking performance 20
2. Particle identification 20

B. Key first-day observables 22
1. Centrality determination 22
2. Centrality determination based on FHCal energy deposition 24
3. Multiplicity yields and ratios of identified charged hadrons 25
4. Mean transverse energy per identified charged hadron 26
5. particle yields (dN/dy) and particle-antiparticle ratios for charged hadrons 27
6. Bulk properties: hadron spectra, yield, and ratios 28
7. (Anti)Λ and Ξ^- reconstruction 29
8. Ξ^+ and $\Omega^{\mp}$ reconstruction 30
9. Reconstruction of resonances 31
10. Directed flow 33
11. Elliptic flow 35
12. Electromagnetic signals 37
13. Two-pion intensity interferometry 39
14. Event-by-event net-proton and net-kaon measurements 41

C. Summary timeline for first-day physics results publication 42

References 43

I. THE NICA COMPLEX CONSTRUCTION SCHEDULE AND EXPECTED INITIAL PERFORMANCE

The NICA Accelerator complex progress is described in detail in XYZ. The expected date of the start of commissioning of NICA accelerator ring is September 2022. The initial luminosity is planned to be at least $10^{24}\ cm^{-2}s^{-1}$ with relatively quick increase to at least $10^{25}\ cm^{-2}s^{-1}$. Symmetric collisions of heavy ions will be performed in the initial stages of NICA operation. Several types of ions are under consideration for the initial NICA operation, including ^{197}Au ions, which were used in previous and ongoing experiments at RHIC in the Beam Energy Scan program, ^{208}Pb ions which were used for extensive data runs at SPS as well as ^{209}Bi ions, which are very similar to Pb ions, but provide more reliable operation of the NICA injection and acceleration complex at the commissioning and first running phase. The expected beam momentum provided by the Nuclotron will be in the range of 2.5 to 3.8 GeV/c^2. At the initial stage additional acceleration of the beams in NICA Collider is not foreseen. Therefore the initial collision energy $\sqrt{s_{NN}}$ may vary from 7 up to 9.46 GeV, with the maximum possible collision energy of 9.46 GeV being preferable.

II. READINESS OF THE MPD EXPERIMENT

The overall structure of the MPD detector in the first stage of data-taking (Stage 1) is shown in Fig. 1.

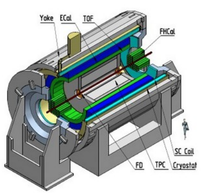

FIG. 1. The overall schematic of the MPD subsystems in the first stage of operation (Stage 1).

A. Technical infrastructure and support systems

1. MPD Hall and facilities

The MPD experiment will be housed in the MPD Hall, which is an integral part of the NICA Accelerator com-

Computing for MPD

Generator	PWG	coll.	$\sqrt{s}$	# of events (10^6)	reco
UrQMD [5]	PWG4	AuAu	11	15	+
		BiBi	9	10	+
		BiBi	9.46	10	+
	PWG2	AuAu	11	10	+
	PWG3	AuAu	7.7	10	+
		BiBi	9	10	+
			7.7	10	+
SMASH [6]	PWG1	AuAu	4/7/9/11	20/20/20/20	-
		ArAr	4/7/9/11	20/20/20/20	-
		XeXe	4/7/9/11	20/20/20/20	-
		CC	4/7/9/11	20/20/20/20	-
		pp	4/7/9/11	50/50/50/50	-
PHQMD [7]	PWG2	BiBi	8.8	15	+

Supercomputer
“GOVORUN”

Fractal analysis of events

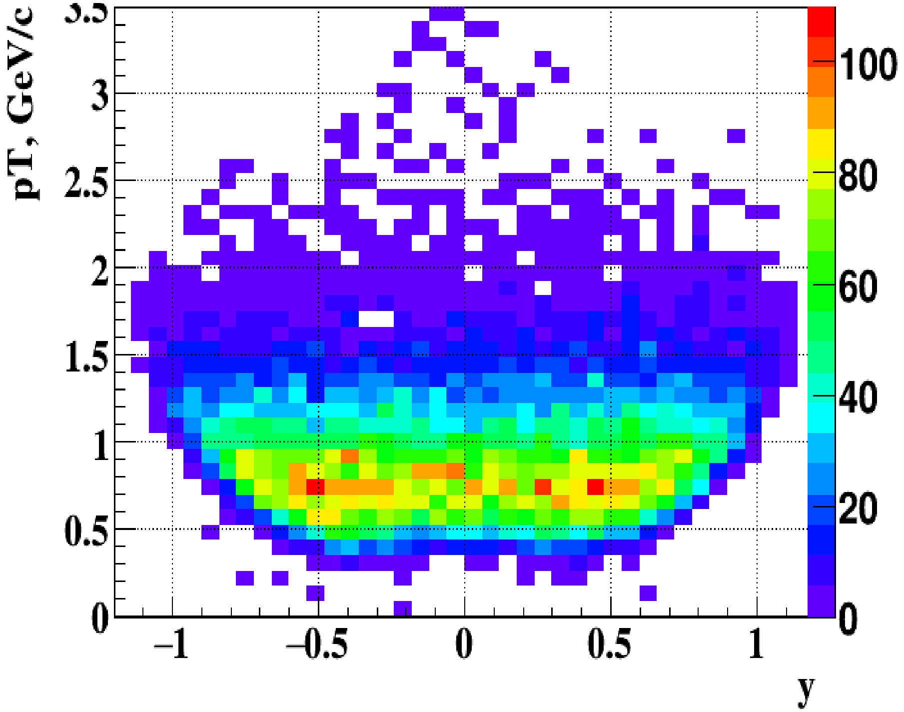

$$D_{bc} = \lim_{\varepsilon \to 0} \frac{\lg N(\varepsilon)}{\lg 1/\varepsilon}$$

N(ε) is the number of boxes of side length ε required to cover the set.

Fractal dimensions in ηP_T space of STAR events for AuAu @ $\sqrt{s}$=200 GeV

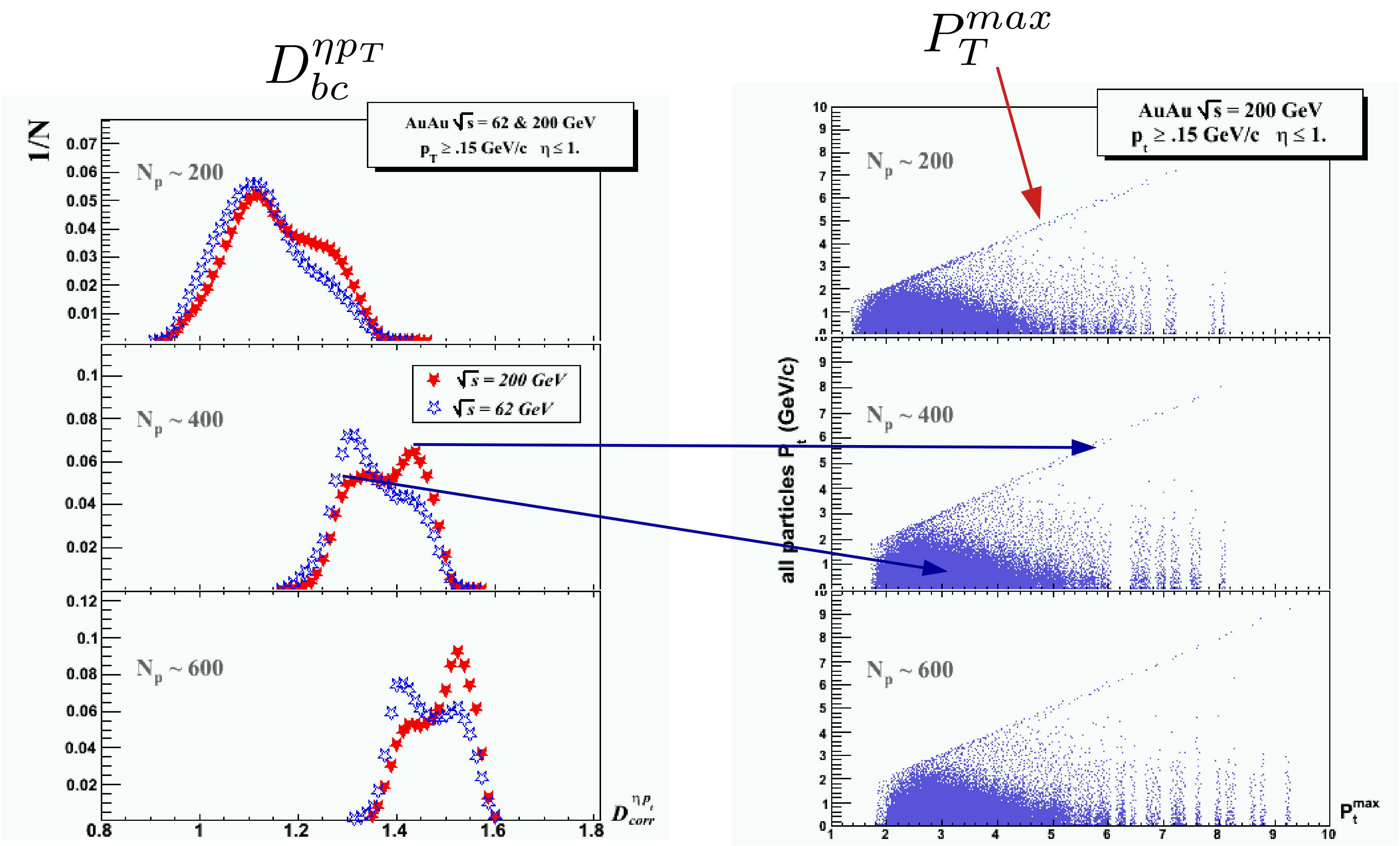

Jet quenching

Phys. Rev. Lett. 91, 072304 (2003).

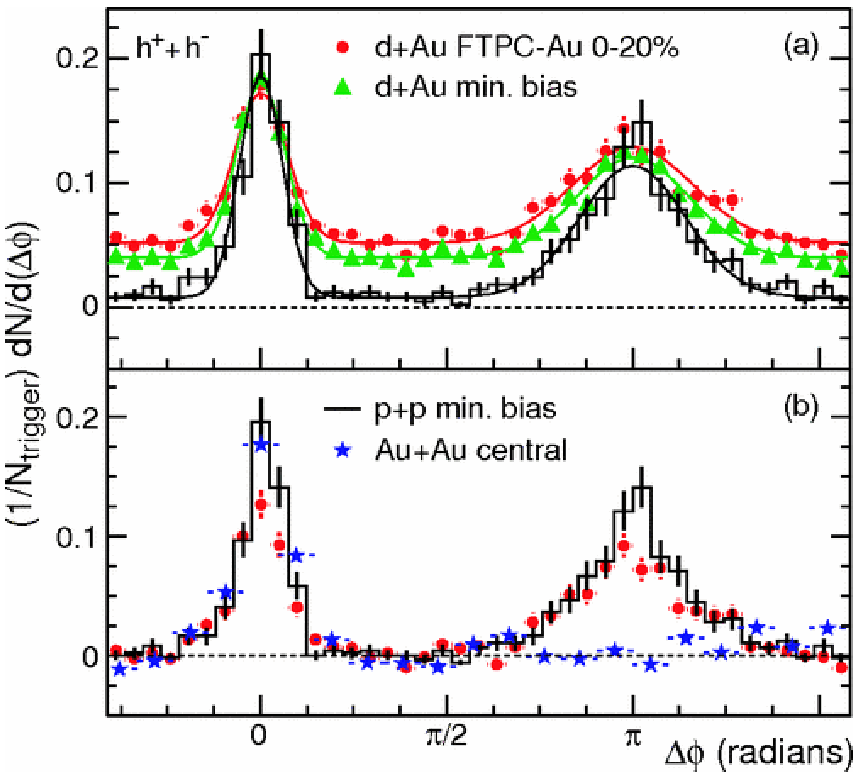

$|\eta| < 0.7$
$4\ \mathrm{GeV}/c < p^{trig}_T < 6\ \mathrm{GeV}/c$
$2\ \mathrm{GeV}/c < p_T^{associated} < p_T^{trig}$

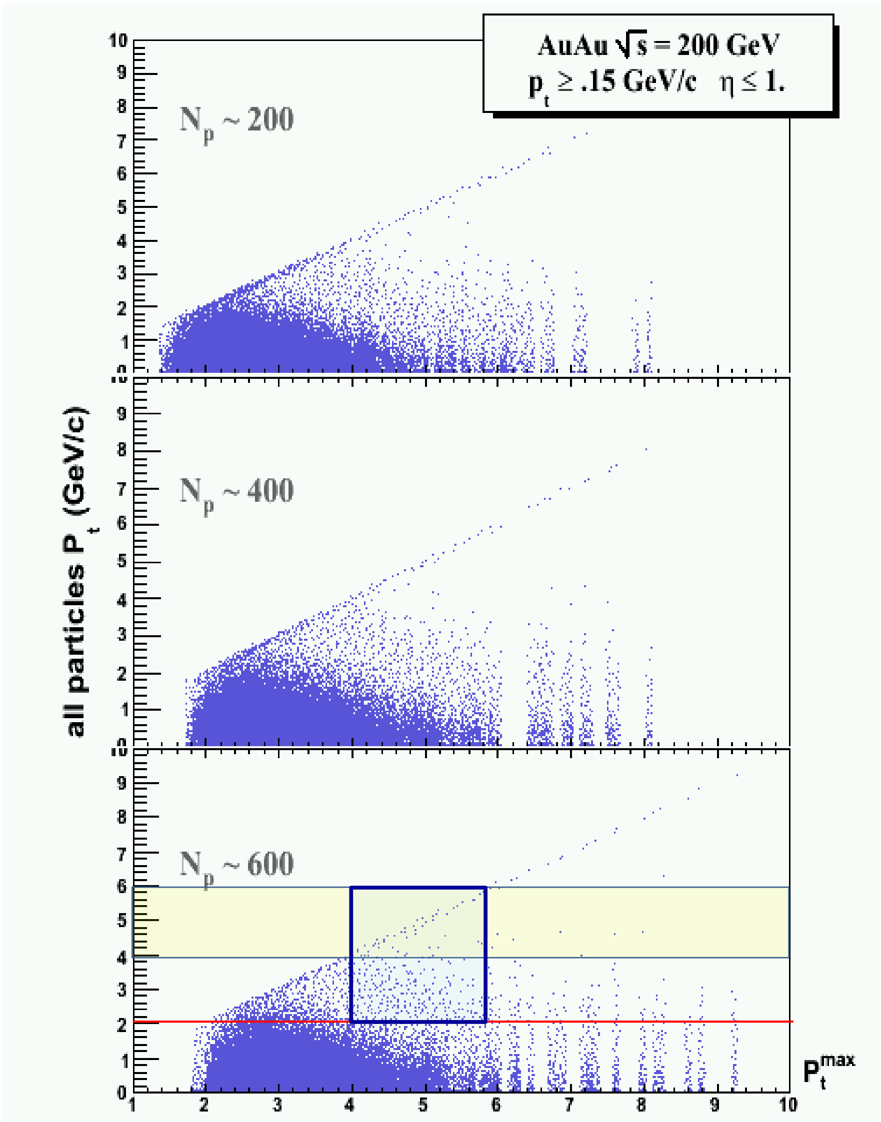

Thanks for attention